

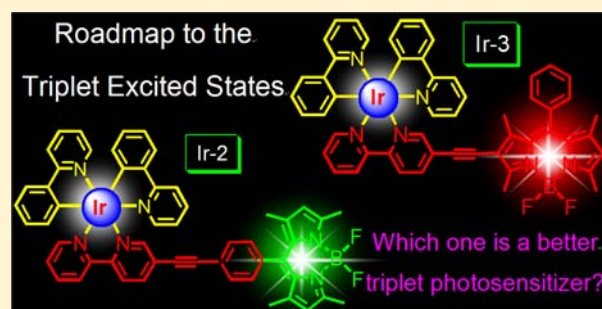
# Efficient Enhancement of the Visible-Light Absorption of Cyclometalated Ir(III) Complexes Triplet Photosensitizers with Bodipy and Applications in Photooxidation and Triplet–Triplet Annihilation Upconversion

Jifu Sun, Fangfang Zhong, Xiuyu Yi, and Jianzhang Zhao\*

State Key Laboratory of Fine Chemicals, School of Chemical Engineering, Dalian University of Technology, E-208 West Campus, 2 Ling Gong Road, Dalian 116024, China

## Supporting Information

**ABSTRACT:** We report molecular designing strategies to enhance the effective visible-light absorption of cyclometalated Ir(III) complexes. Cationic cyclometalated Ir(III) complexes were prepared in which boron–dipyrrromethene (Bodipy) units were attached to the 2,2′-bipyridine (bpy) ligand via  $-C\equiv C-$  bonds at either the *meso*-phenyl (Ir-2) or 2 position of the  $\pi$  core of Bodipy (Ir-3). For the first time the effect of  $\pi$  conjugating (Ir-3) or tethering (Ir-2) of a light-harvesting chromophore to the coordination center on the photophysical properties was compared in detail. Ir(ppy)<sub>2</sub>(bpy) (Ir-1; ppy = 2-phenylpyridine) was used as model complex, which gives the typical weak absorption in visible range ( $\epsilon < 4790 \text{ M}^{-1} \text{ cm}^{-1}$  in region  $> 400 \text{ nm}$ ). Ir-2 and Ir-3 showed much stronger absorption in the visible range ( $\epsilon = 71\,400 \text{ M}^{-1} \text{ cm}^{-1}$  at 499 nm and  $83\,000 \text{ M}^{-1} \text{ cm}^{-1}$  at 527 nm, respectively). Room-temperature phosphorescence was only observed for Ir-1 ( $\lambda_{\text{em}} = 590 \text{ nm}$ ) and Ir-3 ( $\lambda_{\text{em}} = 742 \text{ nm}$ ). Ir-3 gives RT phosphorescence of the Bodipy unit. On the basis of the 77 K emission spectra, nanosecond transient absorption spectra, and spin density analysis, we proposed that Bodipy-localized long-lived triplet excited states were populated for Ir-2 ( $\tau_{\text{T}} = 23.7 \mu\text{s}$ ) and Ir-3 ( $87.2 \mu\text{s}$ ). Ir-1 gives a much shorter triplet-state lifetime ( $0.35 \mu\text{s}$ ). Complexes were used as singlet oxygen ( $^1\text{O}_2$ ) photosensitizers in photooxidation. The  $^1\text{O}_2$  quantum yield of Ir-3 ( $\Phi_{\Delta} = 0.97$ ) is ca. 2-fold of Ir-2 ( $\Phi_{\Delta} = 0.52$ ). Complexes were also used as triplet photosensitizer for TTA upconversion; upconversion quantum yields of 1.2% and 2.8% were observed for Ir-2 and Ir-3, respectively. Our results proved that the strong absorption of visible light of Ir-2 failed to enhance production of a triplet excited state. These results are useful for designing transition metal complexes that show *effective* strong visible-light absorption and long-lived triplet excited states, which can be used as ideal triplet photosensitizers in photocatalysis and TTA upconversion.



## INTRODUCTION

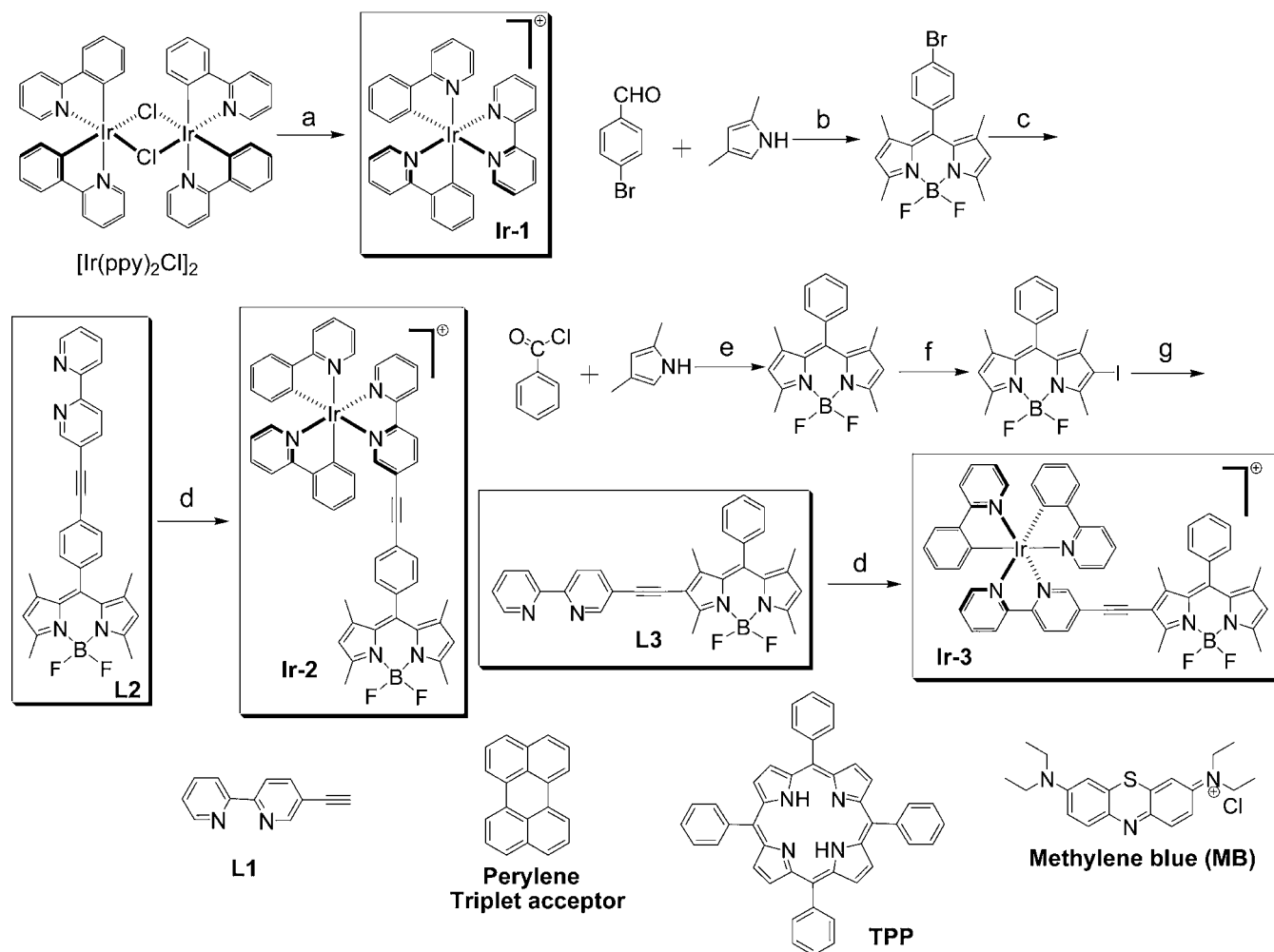
Cyclometalated Ir(III) complexes have attracted much attention owing to their applications in electroluminescence,<sup>1–14</sup> luminescent molecular probes,<sup>15–23</sup> photocatalysis,<sup>24–26</sup> molecular arrays and photoinduced charge separation,<sup>27–30</sup> and more recently triplet–triplet annihilation (TTA) upconversion.<sup>31–33</sup> Normally cyclometalated Ir(III) complexes show *weak* absorption of visible light and *short* triplet excited-state lifetimes ( $\tau$ , a few microseconds).<sup>27,34–38</sup> Conventionally these complexes were used for electroluminescence, but they are *not* suitable for application in the newly developed areas, such as photocatalysis,<sup>24,39,40</sup> luminescent molecular probes,<sup>15,18,20,41</sup> and TTA upconversion,<sup>33</sup> for which strong absorption of visible light or long-lived triplet excited states are desired.<sup>42,43</sup> For example, cyclometalated Ir(III) complexes were used for photocatalysis ( $\text{H}_2$  production and  $^1\text{O}_2$  sensitizing), but these complexes are still limited to those with weak absorption of visible light.<sup>24</sup> Therefore, Ir(III) complexes with strong

absorption of visible light and a long-lived triplet excited state are highly desired.<sup>42,43</sup>

However, simply attaching a visible-light-absorbing organic ligand to the coordination center could not guarantee effective funneling of the excitation energy to the triplet excited state.<sup>16,43–47</sup> For example, 4,4-difluoro-4-bora-3a,4a-diaza-s-indacene (boron–dipyrrromethene, Bodipy) has been seminal used to prepare Ru(II) and Ir(III) complexes,<sup>48,49</sup> but the *effective* absorption of these complexes was not enhanced, that is, the excitation energy harvested by the ligand was not effectively transferred to the triplet-state manifold.<sup>48</sup> A cyclometalated Ir(III) complex with Bodipy on the coordination ligand was reported, but application of the triplet excited state was not studied.<sup>49</sup> The energy-transfer efficiency from the singlet excited state of the ligand to the triplet excited state of

Received: October 10, 2012

Published: January 17, 2013

Scheme 1. Synthesis Routes of Ir-1, Ir-2, and Ir-3<sup>a</sup>

<sup>a</sup>The complexes are cationic, and the counter anion PF<sub>6</sub><sup>-</sup> was omitted for clarity. The molecular structure of the triplet acceptor perylene used in TTA upconversion, the model triplet photosensitizers tetraphenylporphyrin (TPP) and methylene blue (MB) for photooxidation are also shown. (a) 2,2'-Bipyridine, CH<sub>2</sub>Cl<sub>2</sub>/MeOH (2:1, v/v), Ar, reflux, 6 h. (b) Dry CH<sub>2</sub>Cl<sub>2</sub>, CF<sub>3</sub>COOH, DDQ, BF<sub>3</sub>·OEt<sub>2</sub>, NEt<sub>3</sub>, argon, rt. (c) 5-Ethynyl-2,2'-bipyridine, NEt<sub>3</sub>, Pd(PPh<sub>3</sub>)<sub>2</sub>Cl<sub>2</sub>, PPh<sub>3</sub>, CuI, argon, reflux, 8 h. (d) [Ir(ppy)<sub>2</sub>]Cl, CH<sub>2</sub>Cl<sub>2</sub>/MeOH (2:1, v/v), argon, reflux, 6 h. (e) Dry CH<sub>2</sub>Cl<sub>2</sub>, BF<sub>3</sub>·OEt<sub>2</sub>, NEt<sub>3</sub>, argon, rt. (f) NIS (1.0 equiv), rt. (g) 5-Ethynyl-2,2'-bipyridine, NEt<sub>3</sub>, Pd(PPh<sub>3</sub>)<sub>2</sub>Cl<sub>2</sub>, PPh<sub>3</sub>, CuI, argon, 60 °C, 12 h.

the complexes may be evaluated by application of the complexes in triplet-triplet energy-transfer (TTET) process.

Recently, we prepared Ru(II) complexes with a coumarin moiety and showed that the relative energy level of the ligand and coordination center must be matched to ensure efficient energy transfer.<sup>50</sup> However, it is clear that these molecular design strategies need to be generalized with more exemplars.

Herein we demonstrate that the energy transfer from light-absorbing ligand to the triplet excited-state manifold of the Ir(III) complexes can be enhanced by attaching organic chromophores to the coordination center via a  $\pi$ -conjugation linker (C $\equiv$ C triple bond).<sup>43,45,47</sup> With this method, the heavy atom effect of Ir(III) can be maximized and the excitation energy can be efficiently funneled to the triplet excited states. As a result, application of the Ir(III) complexes in photocatalysis or TTA upconversion will be enhanced.

Following this line, we prepared two cyclometalated Ir(III) complexes with Bodipy ligands (Ir-2 and Ir-3, Scheme 1). Ir-2 follows the conventional structural profile, i.e., the  $\pi$  core of the Bodipy chromophore was *not* directly attached to the coordination center.<sup>49</sup> Ir-3, however, follows the direct

metallation concept,<sup>43,47</sup> i.e., the  $\pi$  core of the Bodipy chromophore is directly attached to the Ir(III) coordination center via a  $\pi$ -conjugation linker.<sup>43,45,47</sup> Both Ir-2 and Ir-3 show strong absorption of visible light. Ir-3 shows the room-temperature (RT) phosphorescence of Bodipy, but Ir-2 did not show RT phosphorescence of the Bodipy unit. We found that Ir-3 is more efficient than Ir-2 as triplet photosensitizer in photooxidation and TTA upconversion. Our results may be useful for designing new visible-light-absorbing cyclometalated Ir(III) complexes and applications of these complexes in photocatalysis, photovoltaics, and TTA upconversion.

## RESULTS AND DISCUSSION

**Molecules Design and Synthesis.** The principal molecular design strategy of Ir(III) complexes Ir-2 and Ir-3 is to compare the effect of the different connection profile of the light-harvesting ligand to the coordination center.<sup>43,44,47,49</sup> For Ir-2, Bodipy is connected at the meso phenyl group; thus, the Ir(III) coordination center is isolated from Bodipy.<sup>49</sup> For Ir-3, however, the 2 position of the  $\pi$  core of the Bodipy chromophore is connected to the coordination center via the

C≡C bond.<sup>47</sup> Thus, we expected that the heavy-atom effect in **Ir-3** is more significant than that in **Ir-2**. Bodipy was selected as the light-absorbing ligand owing to its versatile derivatization chemistry, strong absorption of visible light, and good photostability.<sup>51–58</sup>

Preparation of the Bodipy-containing ligands **L2** and **L3** were carried out using Sonogashira coupling reactions. 5-Ethynyl-2,2'-bipyridine was used as the intermediate. Ir(III) complexes were synthesized from the di-Ir(III) intermediate.<sup>59</sup> All complexes were obtained with satisfactory yields (for more detail, see the Experimental Section). **Ir-1** was prepared as the model complex for photophysical studies.

**Steady-State Electronic Spectroscopy (Absorption and Emission).** **L2** shows strong absorption at 499 nm ( $\epsilon = 86\,400\text{ M}^{-1}\text{ cm}^{-1}$ ), which is similar to the Bodipy chromophore (see Figure S29, Supporting Information). For **L3**, however, the absorption is red shifted by 28 nm and  $\epsilon$  decreased to  $58\,500\text{ M}^{-1}\text{ cm}^{-1}$  (Figure 1a). Absorption of **L2** and **L3** shows a

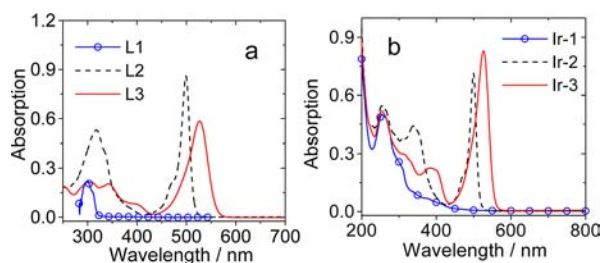


**Figure 1.** (a) UV-vis absorption spectra of ligands **L1**, **L2**, and **L3**. (b) UV-vis absorption spectra of complexes **Ir-1**, **Ir-2**, and **Ir-3**.  $c = 1.0 \times 10^{-5}\text{ M}$  in  $\text{CH}_3\text{CN}$  at  $20\text{ }^\circ\text{C}$ .

substantial difference in the range of 250–400 nm. Absorption of **L3** is red shifted compared to the unsubstituted Bodipy, but **L2** shows a similar absorption band in the visible region to unsubstituted Bodipy (see Figure S29, Supporting Information). Thus, we conclude that the Bodipy unit in **L3** is in  $\pi$  conjugation with bpy ligand but not in **L2**.

**Ir-2** shows the absorption profile in the visible range similar to **L2** (Figure 1b). For **Ir-3**, however, absorption in visible range is enhanced ( $\epsilon = 83\,000\text{ M}^{-1}\text{ cm}^{-1}$  at 527 nm) compared to **L3**. Thus, the electronic interaction between Bodipy and the Ir(III) coordination center is significant for **Ir-3**.<sup>45,46,60,61</sup> **Ir-1** shows absorption in the UV range, which is typical for cyclometalated Ir(III) complexes.<sup>59,62–65</sup> To the best of our knowledge, very few cyclometalated Ir(III) complexes show such intense absorption in the visible range like **Ir-3**.<sup>10,43</sup>

Previously a cyclometalated Ir(III) complex with structure similar to **Ir-2** was reported,<sup>49</sup> but Bodipy-containing Ir(III) complexes similar to the structural profile of **Ir-3** were never reported. A cyclometalated Ir(III) complex with dipyrinato ligands was reported with slightly smaller molar absorption coefficients ( $\epsilon < 38\,400\text{ M}^{-1}\text{ cm}^{-1}$  at 483 nm).<sup>44</sup>

Both of the ligands (**L2** and **L3**) gave intense fluorescence in the visible range (Figure 2a). The fluorescence quantum yields ( $\Phi_F$ ) of **L2** and **L3** were determined as 43.9% and 33.6%, respectively (Table 1). Interestingly, **L3** gives a more red-shifted emission than **L2**. This is an indication that the  $\pi$ -conjugation framework in **L3** is larger than that in **L2**.

**Ir-1** shows broad and structureless emission at 590 nm (Figure 2b).<sup>62</sup> **Ir-2** and **Ir-3** give blue-shifted emission at 514 and 553 nm, respectively. Emission bands of **Ir-2** and **Ir-3** are drastically narrower than that of **Ir-1**. Weak emission at 742 nm was observed for **Ir-3**. The emission wavelengths of **Ir-2** and **Ir-3** are close to emission of **L2** and **L3**. Thus, the major emission bands of **Ir-2** and **Ir-3** were assigned to emission of Bodipy ligands. The minor emission band of **Ir-3** at 742 nm is due to the RT phosphorescence of the Bodipy unit.<sup>47–49</sup> RT phosphorescence of the Bodipy unit was not observed for **Ir-2**. Furthermore, upon excitation at 507 nm, where both complexes **Ir-2** and **Ir-3** show the same  $\epsilon$  value, much weaker fluorescence was observed for **Ir-3** than that for **Ir-2** (Figure 2c).

The emission properties of the complexes were studied under different atmospheres (Figure 3). For **Ir-1**, the broad, structureless emission band can be quenched by 81.6% in aerated solution compared to that in deaerated solution. In  $\text{O}_2$ -saturated solution, emission was quenched by 95.3%. This is typical for phosphorescent complexes.<sup>63–66</sup> The luminescence lifetime of **Ir-1** was determined as 0.30  $\mu\text{s}$ , which confirmed the phosphorescence feature of the emission of **Ir-1**.

In contrast to **Ir-1**, emission of **Ir-2** is not sensitive to  $\text{O}_2$  (Figure 3b). The luminescence lifetime of **Ir-2** was determined as 0.9 ns; the Stokes shift is small (15 nm,  $585\text{ cm}^{-1}$ ), which confirmed the fluorescence feature of the emission. As proof, the emission lifetime of **Ir-2** is much shorter than the free ligand **L2** (1.9 ns). Fluorescence of the ligand in **Ir-2** was quenched ( $\Phi_F = 1.8\%$ ), compared to the free ligand **L2** ( $\Phi_F = 43.9\%$ ).

The  $\text{O}_2$  sensitivity of the emission bands confirms that the emission of **Ir-3** at 553 nm is due to the fluorescence, but the emission at 742 nm is phosphorescence (Figure 3c).<sup>13</sup> Previously a Bodipy-containing cyclometalated Ir(III) complex was reported, but the phosphorescence of Bodipy can be

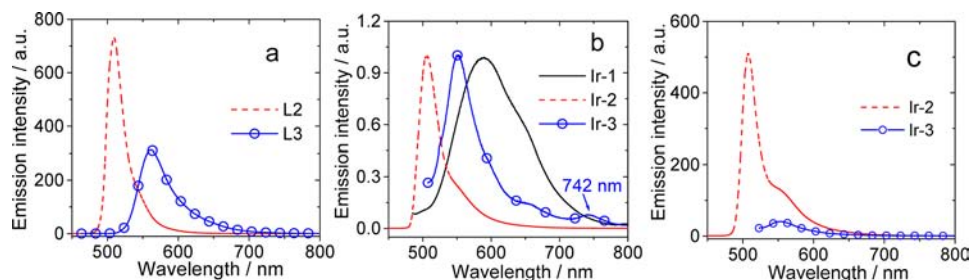


**Figure 2.** (a) Emission spectra of ligands **L2** ( $\lambda_{\text{ex}} = 500\text{ nm}$ ) and **L3** ( $\lambda_{\text{ex}} = 510\text{ nm}$ ),  $c = 1.0 \times 10^{-6}\text{ M}$  in  $\text{CH}_3\text{CN}$  at  $20\text{ }^\circ\text{C}$ . (b) Normalized emission spectra of complexes **Ir-1** ( $\lambda_{\text{ex}} = 410\text{ nm}$ ), **Ir-2** ( $\lambda_{\text{ex}} = 500\text{ nm}$ ), and **Ir-3** ( $\lambda_{\text{ex}} = 510\text{ nm}$ ); note the RT phosphorescence of **Ir-3** ( $\lambda_{\text{em}} = 742\text{ nm}$ ),  $c = 1.0 \times 10^{-6}\text{ M}$  in  $\text{CH}_3\text{CN}$  at  $20\text{ }^\circ\text{C}$ . (c) Comparison of the emission intensity of complexes **Ir-2** and **Ir-3** under the same conditions ( $\lambda_{\text{ex}} = 507\text{ nm}$ ; the absorbance of both **Ir-2** and **Ir-3** at 507 nm is 0.06).

Table 1. Photophysical Properties of the Ligands and Cyclometalated Ir(III) Complexes

compounds	$\lambda_{\text{abs}}/\text{nm}^a$	$\epsilon^b$	$\lambda_{\text{em}}/\text{nm}^c$	$\Phi/\%^d$	triplet-state lifetime <sup>e</sup>		luminescence lifetime	
					$\tau_T/\mu\text{s}/(\text{N}_2)$	$\tau_T/\text{ns}/(\text{air})$	$\tau_L/(\text{RT})^f$	$\tau_L/(77\text{ K})^g$
L2	499	8.64	512	43.9	<i>h</i>	<i>h</i>	1.9 ns	<i>h</i>
L3	527	5.85	565	33.6	<i>h</i>	<i>h</i>	3.5 ns	<i>h</i>
Ir-1	255	4.99	590	4.5	0.35	57.8	0.30 $\mu\text{s}$	4.8 $\mu\text{s}$
Ir-2	499	7.14	514	1.8	23.7	264.6	0.9 ns	2.8 ns
Ir-3	527	8.30	553/742	0.3/0.03	87.2	303.3	2.6 ns/ <sup><i>i</i></sup>	3.9 ns/4.5 ms

<sup>a</sup>Maxima UV–vis absorption wavelength in CH<sub>3</sub>CN (1.0 × 10<sup>−5</sup> M, 20 °C). <sup>b</sup>Molar absorption coefficient at absorption maxima.  $\epsilon = 10^4\text{ M}^{-1}\text{ cm}^{-1}$ . <sup>c</sup>Maxima emission wavelength in CH<sub>3</sub>CN (1.0 × 10<sup>−5</sup> M, 20 °C). <sup>d</sup>Luminescence quantum yields in CH<sub>3</sub>CN (20 °C) with complex Ru(dmb)<sub>3</sub>[PF<sub>6</sub>]<sub>2</sub> ( $\Phi_p = 7.3\%$  in CH<sub>3</sub>CN) and 2,6-diiodo-1,3,5,7-tetramethyl-8-phenyl-4,4-difluoroboradiazaindacene ( $\Phi_F = 2.7\%$  in CH<sub>3</sub>CN) as standard. <sup>e</sup>Measured by transient absorption in CH<sub>3</sub>CN (1.0 × 10<sup>−5</sup> M, 20 °C). <sup>f</sup>In CH<sub>3</sub>CN (1.0 × 10<sup>−5</sup> M, 20 °C). <sup>g</sup>In EtOH/MeOH (4:1, v/v, 1.0 × 10<sup>−5</sup> M). <sup>h</sup>Not applicable. <sup>i</sup>Too weak to be determined accurately.

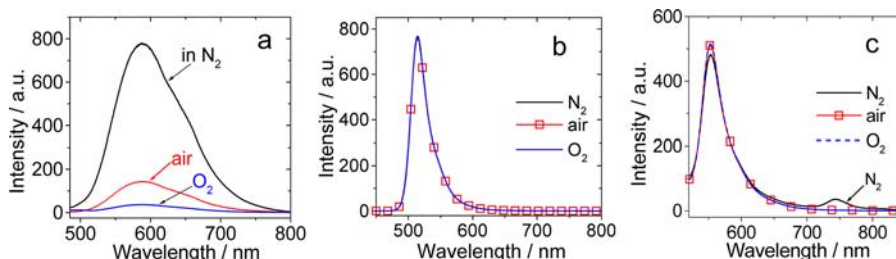


Figure 3. Emission spectra of the complexes in N<sub>2</sub>-, air-, and O<sub>2</sub>-saturated solution. (a) Ir-1 ( $\lambda_{\text{ex}} = 410\text{ nm}$ ,  $\lambda_{\text{em}} = 590\text{ nm}$ ). (b) Ir-2 ( $\lambda_{\text{ex}} = 500\text{ nm}$ ,  $\lambda_{\text{em}} = 514\text{ nm}$ ). (c) Ir-3 ( $\lambda_{\text{ex}} = 510\text{ nm}$ ,  $\lambda_{\text{em}} = 553\text{ and }742\text{ nm}$ ).  $c = 1.0 \times 10^{-5}\text{ M}$  in CH<sub>3</sub>CN at 20 °C.

observed only at 77 K.<sup>49</sup> The photophysical properties of the ligands and cyclometalated Ir(III) complexes are listed in Table 1.

Excitation spectra of the complexes were also studied (Supporting Information, Figure S30). For Ir-2, the MLCT absorption band is less efficient than the Bodipy band to produce the Bodipy ligand fluorescence. Therefore, we propose that the energy transfer from the <sup>1</sup>MLCT\* state to the <sup>1</sup>Bodipy\* state is nonefficient, possibly due to the lower energy level of the relaxed <sup>1</sup>MLCT\* state than the <sup>1</sup>Bodipy\* state or the fast <sup>1</sup>MLCT\* → <sup>3</sup>MLCT\* process; therefore, <sup>1</sup>MLCT\* → <sup>1</sup>Bodipy\* is nonefficient. It should be pointed out that it is difficult to study the energy level of the relaxed <sup>1</sup>MLCT\* state (note it is not the excitation energy gap), which is nonluminescent due to the fast <sup>1</sup>MLCT\* → <sup>3</sup>MLCT\* process. For Ir-3, similar results were observed (Figure S30, Supporting Information). The excitation spectrum with an emission wavelength at 742 nm was also recorded. We found that the Bodipy absorption band in the region of 450–600 nm is efficient to produce the emission at 742 nm, which is similar to the MLCT absorption band. Therefore, we propose that both the <sup>3</sup>MLCT → <sup>3</sup>Bodipy\* and <sup>1</sup>Bodipy\* → <sup>3</sup>Bodipy\* processes are efficient.

**Nanosecond Time-Resolved Transient Difference Absorption Spectroscopy.** In order to study the triplet excited state of the complexes, the nanosecond time-resolved transient difference absorption spectra were studied (Figure 4). Upon pulsed laser excitation, transient absorption (TA) bands at 378 and 763 nm were observed for Ir-1 (Figure 4a). The bleaching band at 618 nm is due to the phosphorescence of Ir-1 (Figure 2b). The lifetime was 0.35  $\mu\text{s}$  (Figure 4b).

For Ir-3, the positive transient absorption in the range of 600–750 nm is more significant than Ir-1 (Figure 4c). The bleaching band for Ir-3 is located at 526 nm, which is in good agreement with the steady-state absorption (Figure 1b). Thus,

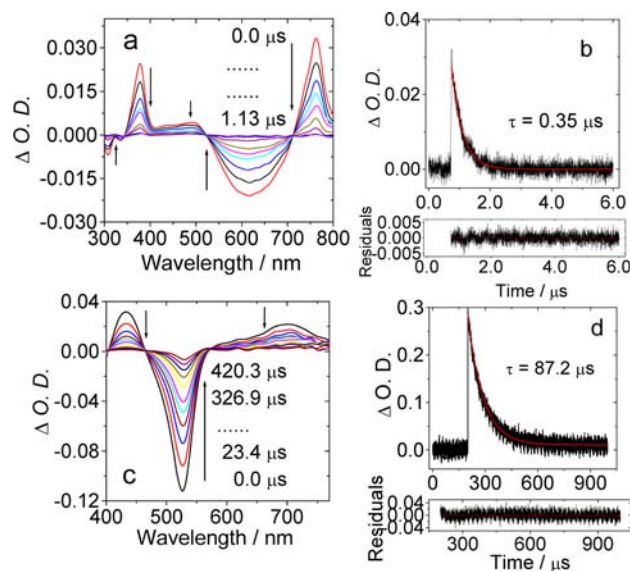
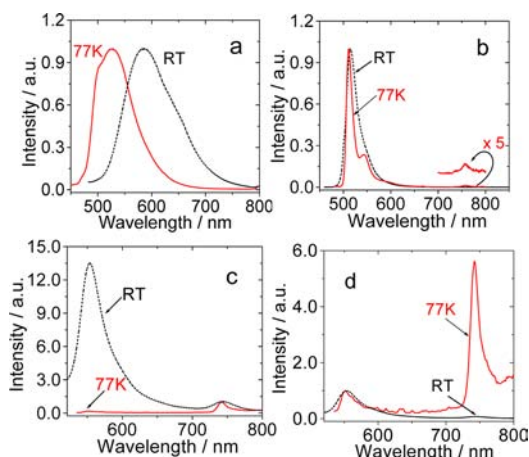


Figure 4. Nanosecond time-resolved transient difference absorption spectra: (a) Ir-1 ( $\lambda_{\text{ex}} = 355\text{ nm}$ ); (b) decay trace of Ir-1 at 610 nm; (c) Ir-3 ( $\lambda_{\text{ex}} = 532\text{ nm}$ ); (d) decay trace of Ir-3 at 530 nm.  $c = 1.0 \times 10^{-5}\text{ M}$  in deoxygenated CH<sub>3</sub>CN at 20 °C.

the triplet excited state of Ir-3 is localized on the Bodipy ligand, not on the Ir(III) coordination center. The lifetime of Ir-3 was determined as 87.2  $\mu\text{s}$ , much longer than Ir-1 (0.35  $\mu\text{s}$ ).

The TA spectrum of Ir-2 is similar to that of Ir-3, with the bleaching band in the slightly blue-shifted range (see Figure S33, Supporting Information). The lifetime of the transient was determined as 23.7  $\mu\text{s}$  (Table 1), which is close to a similar Bodipy-containing Ir(III) complex (25  $\mu\text{s}$ ).<sup>49</sup>

**Emission Spectra at 77 K.** The luminescence of the complexes at 77 K was studied (Figure 5). For Ir-1, the emission is broad and structureless at 77 K, which is similar to



**Figure 5.** Normalized emission spectra of the Ir(III) complexes at RT (20 °C) and 77 K in EtOH/MeOH mixed solvent (4:1, v/v): (a) Ir-1,  $\lambda_{\text{ex}} = 405$  nm; (b) Ir-2,  $\lambda_{\text{ex}} = 500$  nm; (c) Ir-3,  $\lambda_{\text{ex}} = 510$  nm, spectra were normalized at 742 nm; (d) Ir-3,  $\lambda_{\text{ex}} = 510$  nm, fluorescence of Ir-3 at 553 nm is normalized, indicating the greatly increased phosphorescence at 77 K.  $c = 1.0 \times 10^{-5}$  M.

that at RT (Figure 5a). However, the emission at 77 K is blue shifted by 62 nm compared to that at RT. This large thermally induced Stokes shift ( $\Delta E_{\text{S}} = 2100 \text{ cm}^{-1}$ ) is an indication of the  $^3\text{MLCT}$  feature of the emissive triplet excited state of Ir-1.<sup>32</sup>

The luminescence of Ir-2 at 77 K is located at 511 nm, which is very close to that at RT. The luminescence lifetime at 77 K is 2.8 ns, compared to that at RT (0.9 ns). The lifetime suggests that the emission is fluorescence not phosphorescence. Furthermore, a minor emission band at 757 nm was observed at 77 K. This emission band is most probably due to the phosphorescence of the Bodipy unit.<sup>49</sup>

Emission of Ir-3 at 77 K is drastically different from that at RT (Figure 5c and 5d). The emission band at 553 nm becomes much weaker than the emission band at 742 nm. The lifetime of the emission band at 742 nm was determined as 4.5 ms at 77 K; it is an indication of the phosphorescence of the organic chromophore.<sup>67,68</sup>

**Spin Density Surfaces of the Complexes.** The spin density of the lowest-lying triplet state can be indicated by the localization of the spin density of the complexes.<sup>32,43–47,50</sup>

The spin density of Ir-1 is localized on ppy and bpy as well as the Ir(III) atom (Figure 6). This spin density profile is in agreement with the MLCT/IL triplet excited state of Ir(ppy)<sub>2</sub>(bpy).<sup>62</sup> For Ir-2, however, the spin density is mainly localized on the Bodipy ligand; the Ir(III) center and the bpy ligands make little contribution. Thus, the  $T_1$  excited state of Ir-

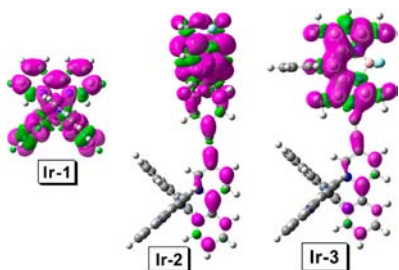
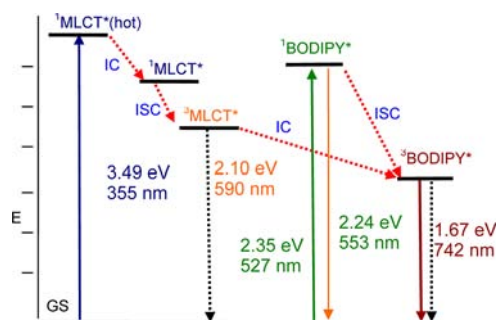


**Figure 6.** Isosurfaces of the spin density of Ir-1, Ir-2, and Ir-3 at the optimized  $T_1$  excited-state geometry (isovalue  $\pm 0.0004$ ) calculated at the B3LYP/6-31G/LANL2DZ level with Gaussian 09W.

2 can be recognized as a Bodipy-localized  $^3\text{IL}$  state.<sup>49</sup> This conclusion is in agreement with the time-resolved transient difference absorption spectroscopy (Figure S33, Supporting Information, and Figure 4) as well as quenching of the MLCT emission of the coordination center in Ir-2 and Ir-3 (Figure 2 and Scheme 2) because Bodipy shows a  $T_1$  state with a much

### Scheme 2. Qualitative Jablonski Diagram for the Photophysical Process of the Ir(III) Complexes Exemplified with Ir-3<sup>a</sup>



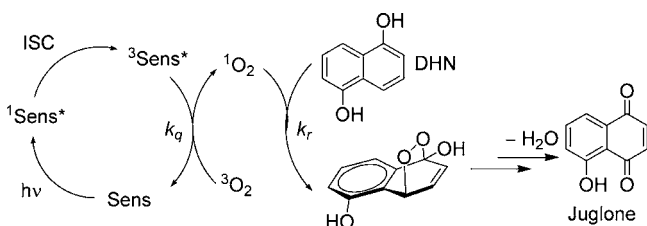
<sup>a</sup>Solid lines represent excitation or radiative decay; dotted lines represent non-radiative processes. Note the  $^3\text{MLCT}$  phosphorescence is quenched by the low-lying  $^3\text{Bodipy}^*$  state. IC stands for internal conversion, and ISC stands for intersystem crossing.

lower energy level than the Ir(III) MLCT state. Similar spin density was observed for Ir-3 (Figure 6). Thus, different from Ir-1, the  $T_1$  excited states of both Ir-2 and Ir-3 can be identified as a  $^3\text{IL}$  excited state. This conclusion is in full agreement with the transient absorption spectroscopy.

The photophysical processes involved in the Ir(III) complexes can be illustrated in Scheme 2. For Ir-1, the  $^1\text{MLCT}^*$  state is populated upon photoexcitation. With the heavy-atom effect of the Ir(III) atom, the  $^3\text{MLCT}^*$  excited state is populated. The  $^3\text{MLCT}^*$  state is emissive; thus, Ir-1 gives phosphorescence. For Ir-2, the  $^1\text{Bodipy}^*$  state energy level is lower than that of the  $^1\text{MLCT}^*$  state (resides on the Ir<sup>III</sup> coordination center). However, based on the excitation spectrum, the  $^1\text{MLCT} \rightarrow ^1\text{IL}$  internal conversion is non-efficient. Thus, the energy transfer from the  $^1\text{Bodipy}^*$  state to the  $^1\text{MLCT}^*$  state is frustrated; the population of the  $^3\text{Bodipy}^*$  state is dependent on the ISC capability of the complexes.<sup>50</sup> The ISC efficiency for the transformation from the  $^1\text{Bodipy}^*$  state to the  $^3\text{Bodipy}^*$  state can be indicated either by the residual fluorescence of the Bodipy unit or the property of the  $^3\text{Bodipy}^*$ , such as the emissive or nonemissive feature.

**Photooxidation of 1,5-Dihydroxynaphthalene with the Ir(III) Complexes as Singlet Oxygen ( $^1\text{O}_2$ ) Photosensitizer.** Next, we will use singlet oxygen ( $^1\text{O}_2$ ) photosensitizing to study the efficiency of producing the  $^3\text{Bodipy}^*$  triplet excited state in Ir-2 and Ir-3.

To evaluate the  $^1\text{O}_2$ -producing capability of the Ir(III) complexes, 1,5-dihydroxynaphthalene (DHN) was used as the  $^1\text{O}_2$  scavenger (Scheme 3).<sup>26,69,70</sup> DHN can be oxidized by  $^1\text{O}_2$  to produce juglone, which is a versatile intermediate for preparation of antitumor reagents.<sup>71</sup> Previously, production of naphthoquinone is based on catalytic oxidation of naphthalene, which is not environmentally benign. Photooxidation of DHN can be monitored by the decrease of the absorption of DHN at 301 nm. The velocity of the photooxidation is proportional to the capability of  $^1\text{O}_2$  production. Previously, conventional

**Scheme 3. Mechanism of the Photooxidation of DHN with a Singlet Oxygen ( $^1\text{O}_2$ ) Photosensitizer<sup>26</sup>**


Ir(III) complexes were used for  $^1\text{O}_2$  photosensitizing.<sup>26</sup> However, those complexes show very weak absorption of visible light, which is the disadvantage of conventional Ir(III) complexes.

The Ir(III) complexes were used as triplet photosensitizers for photooxidation of DHN (Figure 7). More significant

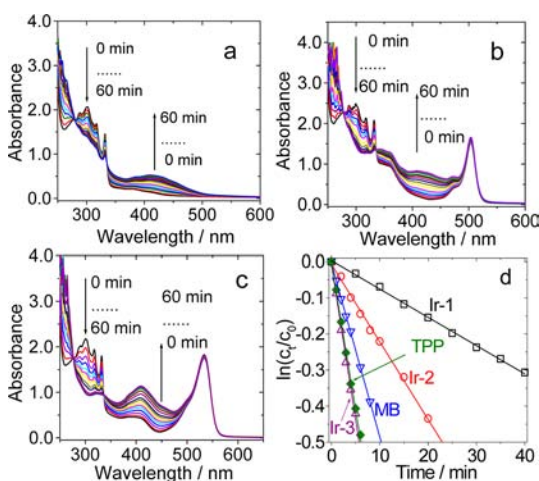


**Figure 7.** Photooxidation of DHN using Ir(III) complexes, MB, and TPP as  $^1\text{O}_2$  photosensitizers. Change of UV-vis absorption spectra using Ir-1 (a), Ir-2 (b), and Ir-3 (c) as sensitizers. (d) Plots of  $\ln(C_t/C_0)$  against irradiation time ( $t$ ) for photooxidation. Irradiated with a 35 W xenon lamp ( $20 \text{ mW cm}^{-2}$  at the photoreactor).  $c$  [photosensitizer] =  $2.0 \times 10^{-5} \text{ M}$  in  $\text{CH}_2\text{Cl}_2/\text{CH}_3\text{OH}$  (9:1, v/v) at  $20^\circ\text{C}$ .

photooxidation with Ir-2 and Ir-3 as  $^1\text{O}_2$  photosensitizer was observed than that with Ir-1. Photooxidation of DHN with different  $^1\text{O}_2$  photosensitizers can be quantitatively compared by plotting  $\ln(C_t/C_0)$  against the irradiation time. Oxidation rate constants can be derived from the slope of the curves (Figure 7d).<sup>26</sup> On the basis of the results, Ir-2 and Ir-3 are more efficient  $^1\text{O}_2$  photosensitizers than Ir-1 due to the weak absorption of Ir-1 in the visible range. Therefore, production of juglone with Ir-2 and Ir-3 is more efficient than that with Ir-1 as the triplet photosensitizer.

Interestingly, the  $K_{\text{obs}}$  value of Ir-3 is 4-fold of Ir-2. The large  $K_{\text{obs}}$  value of Ir-3 may indicate that the ISC of Ir-3 is more efficient than that of Ir-2. The performance of Ir-3 is much better than a known triplet photosensitizer methylene blue (MB) (Figures 7 and 8 and Table 2).

The yields of the photooxidation with different photosensitizers were studied (Figure 8). Ir-3 is more efficient than Ir-2. Moreover, the chemical yield of juglone with Ir-3 as the triplet photosensitizer is higher than that with Ir-2.  $^1\text{O}_2$  quantum yields ( $\Phi_\Delta$ ) of the different triplet photosensitizers

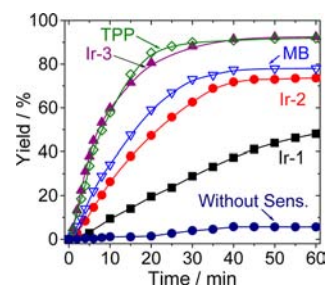


**Figure 8.** Plots of chemical yields of juglone vs irradiation time for photooxidation of DHN using Ir (III) complexes, MB, and TPP as  $^1\text{O}_2$  photosensitizers.

**Table 2. Photophysical and Photooxidation of DHN-Related Parameters of the Ir(III) Complexes, MB, and TPP, Measured in  $\text{CH}_2\text{Cl}_2/\text{CH}_3\text{OH}$  (9:1, v/v) mixed solvent ( $20^\circ\text{C}$ )**

	$\lambda_{\text{abs}}^a$ nm	$\epsilon^b$	$\tau_T^c$ μs	$k_{\text{obs}}^d$	$\nu_i^e$	$\Phi_\Delta^f$	yield (%) <sup>g</sup>
Ir-1	256	50 700	0.35	7.8	15.6	0.92 <sup>g</sup>	37.4
Ir-2	504	75 590	23.7	21.5	43.0	0.52 <sup>h</sup>	71.8
Ir-3	534	95 380	87.2	85.5	171.0	0.97 <sup>h</sup>	91.4
MB	656	131 030	83.3	48.1	96.2	0.57	77.4
TPP	416	284 360	82.5	81.1	162.2	0.65	90.9

<sup>a</sup>Absorption maxima. <sup>b</sup>Molar absorption coefficient at the absorption maxima.  $\epsilon = \text{M}^{-1} \text{ cm}^{-1}$ . <sup>c</sup>Triplet excited-state lifetimes; measured by nanosecond time-resolved transient absorption,  $20^\circ\text{C}$ . <sup>d</sup>Pseudo-first-order rate constant,  $\ln(C_t/C_0) = -k_{\text{obs}}t$ . In  $10^{-3} \text{ min}^{-1}$ . <sup>e</sup>Initial consumption rate of DHN,  $\nu_i = k_{\text{obs}}[\text{DHN}]$ . In  $10^{-7} \text{ M min}^{-1}$ . <sup>f</sup>Singlet oxygen ( $^1\text{O}_2$ ) generation quantum yield. <sup>g</sup>Literature value  $\Phi_\Delta = 0.97$ .<sup>26</sup> <sup>h</sup>Measured in methanol using Rose Bengal (RB,  $\Phi_\Delta = 0.80$  in  $\text{CH}_3\text{OH}$ ) as a reference. <sup>i</sup>Chemical yield of juglone after photoreaction for 40 min.

were also determined (Table 2). The  $\Phi_\Delta$  value of Ir-3 ( $\Phi_\Delta = 97\%$ ) is almost 2-fold of Ir-2 ( $\Phi_\Delta = 52\%$ , Table 2).

**Triplet-Triplet Annihilation Upconversion.** The complexes described herein were used as triplet photosensitizers for another triplet-triplet energy-transfer (TTET) process, i.e., TTA upconversion. TTA upconversion has attracted much attention due to its advantage over other upconversion methods,<sup>33,72–80</sup> such as upconversion with two-photon absorption dyes<sup>81</sup> or rare earth materials.<sup>82–85</sup> TTA upconversion requires triplet photosensitizer for absorbing of the excitation energy and triplet acceptor for the upconverted emission. The energy is transferred from the photosensitizer to the acceptor by TTET process; then the singlet excited state of the acceptor will be produced and the fluorescence from the acceptor can be observed. Previously, a cyclometalated Ir(III) complex, with weak absorption in the visible range, was used as a triplet photosensitizer for TTA upconversion.<sup>31</sup> Recently, we reported coumarin-containing Ir(III) complexes as triplet photosensitizers for TTA upconversion<sup>32</sup> as well as some organic triplet photosensitizers.<sup>86</sup> To the best of our knowledge, strong absorption of Bodipy in visible range has not been used in Ir(III) complexes for TTA upconversion.

Upon 532 nm laser excitation (Figure 9), the complexes give emission similar to that observed in Figure 2. Upon addition of perylene, blue emission in the 445–470 nm range was observed with Ir-3 as the triplet photosensitizer. Excitation of the photosensitizer or acceptor perylene alone at 532 nm did not produce any blue emission band. Thus, TTA upconversion was

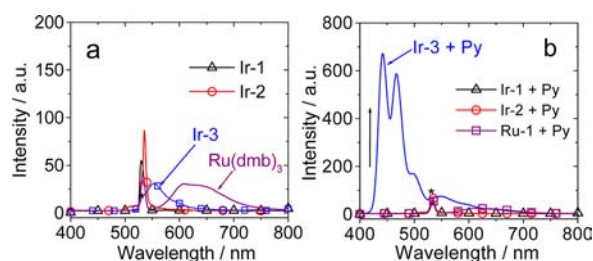


**Figure 9.** Upconversion with Ir-1, Ir-2, Ir-3, and Ru(dmb)<sub>3</sub>[PF<sub>6</sub>]<sub>2</sub> (Ru-1) as triplet sensitizers and perylene (Py) as triplet acceptor, excited by a 532 nm laser (continuous wave, 70 mW cm<sup>-2</sup>). (a) Emission of the complexes alone with a 532 nm laser excitation. (b) Upconversion emission of the mixtures of the sensitizers and perylene upon selective excitation of sensitizers with a 532 nm laser. *c* [sensitizers] = 1.0 × 10<sup>-5</sup> M and *c* [perylene] = 5.0 × 10<sup>-5</sup> M in deaerated CH<sub>3</sub>CN at 20 °C.

confirmed. No upconversion was observed with Ir-2 or Ir-1 as the triplet photosensitizer due to the unmatched excitation wavelength. The TTA upconversion quantum yield ( $\Phi_{UC}$ ) with Ir-3 as the triplet photosensitizer was determined as 2.8%. Considering the strong absorption of Ir-3, the upconversion capability is significant.

We found that TTA upconversion can be observed with excitation of Ir-3 by ambient light (noncoherent), for example, the excitation light from a spectrofluorometer (Figure 10). We

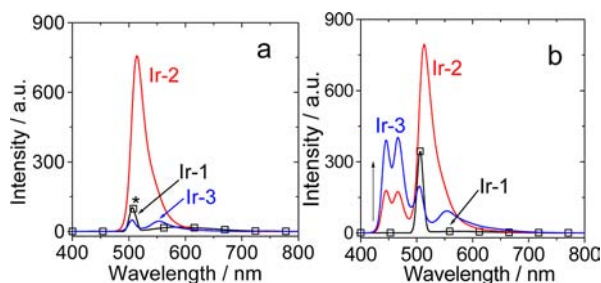


**Figure 10.** Upconversion excited by a spectrofluorometer (507 nm, noncoherent, 4.5 mW cm<sup>-2</sup>) with Ir-2 and Ir-3 as triplet sensitizers and perylene as triplet acceptor. Ir-2 and Ir-3 give the same absorbance at 507 nm ( $A = 0.44$ ). (a) Emission spectra of photosensitizers alone. (b) Upconversion emission spectra of mixtures of the sensitizers and acceptor. *c* [sensitizers] = 1.0 × 10<sup>-5</sup> M and *c* [perylene] = 5.0 × 10<sup>-5</sup> M in deaerated CH<sub>3</sub>CN at 20 °C.

selected 507 nm as the excitation wavelength at which both Ir-2 and Ir-3 show the same  $\epsilon$  value. Thus, the TTA upconversion of Ir-2 and Ir-3 can be compared *directly* by the upconverted emission intensity. The upconverted emission intensity with Ir-3 as the triplet photosensitizer is almost 2-fold of Ir-2 (Figure 10b). This result indicated that the triplet excited state of Ir-3 is more efficiently populated than Ir-2. Herein the  $T_1$  state lifetime will not have a substantial difference on the upconversion quantum yield because the lifetimes of both Ir-2 and Ir-3 are much longer than the required lifetime for an efficient diffusion-controlled process.<sup>76a,b,77</sup>

In order to confirm the TTA upconversion, the luminescence lifetimes of the blue emission in the TTA upconversion experiments were measured (Figure 11). The luminescence lifetime was determined as 19.4  $\mu$ s with Ir-3 as the triplet photosensitizer. In a different experiment, the lifetime of the prompt fluorescence of perylene was determined as 4.0 ns. The exceptionally long-lived lifetime of luminescence confirmed that

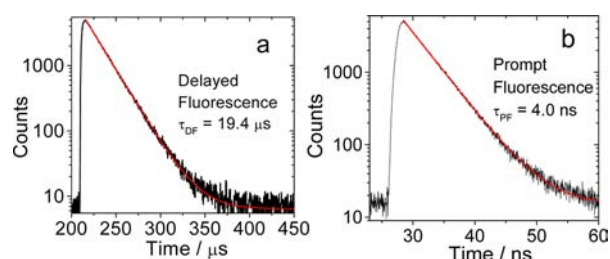


**Figure 11.** (a) Delayed fluorescence of perylene with Ir-3 as triplet photosensitizer for TTA upconversion. Ir-3 was selectively excited at 532 nm, and decay of the emission of perylene was monitored at 445 nm. (b) Prompt fluorescence decay of perylene determined in a different experiment (excited with a picosecond 405 nm laser, decay of the emission at 445 nm was monitored). *c* [Sensitizers] = 1.0 × 10<sup>-5</sup> M and *c* [Perylene] = 5.0 × 10<sup>-5</sup> M in deaerated CH<sub>3</sub>CN at 20 °C.

the emission in the upconversion experiment is the *delayed* fluorescence, which is characteristic for the TTA upconversions.<sup>75,86b,c</sup> Thus, TTA upconversion with Ir-3 as the triplet photosensitizer was unambiguously confirmed. Similarly delayed fluorescence was observed with Ir-2 as the triplet photosensitizer (see Figure S47, Supporting Information).

In order to study the TTET efficiency of TTA upconversion, quenching of the triplet excited states of the photosensitizers by triplet acceptor perylene was studied (Figure 12). The  $K_{SV}$

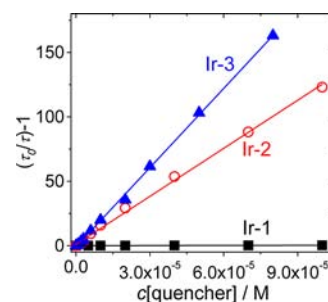


**Figure 12.** Stern–Volmer plots generated from triplet excited-state lifetime ( $\tau_T$ ) quenching of Ir-1, Ir-2, and Ir-3 measured as a function of the concentration of quencher (perylene). Triplet-state lifetimes ( $\tau_T$ ) were measured by nanosecond time-resolved transient difference absorption ( $\lambda_{ex} = 532$  nm) *c* [sensitizers] = 1.0 × 10<sup>-5</sup> M in deaerated CH<sub>3</sub>CN at 20 °C.

value of Ir-3 is ca. 1000-fold of Ir-1. The quenching constant for Ir-3 is 2-fold of Ir-2 (Table 3). The efficient TTET of Ir-3

**Table 3.** Upconversion-Related Parameters of the Ir(III) Complexes and Ru-1<sup>a</sup>

sensitizers	$\Phi_{UC}/(\%)^b$	$K_{sv}/(10^3 M^{-1})^c$	$k_q/(10^9 M^{-1} s^{-1})^f$	$\tau_{DF}/\mu s^g$
Ir-1	0.3 <sup>c</sup>	2.8	8.0	128.8
Ir-2	1.2 <sup>c</sup>	1243.4	52.5	21.3
Ir-3	2.8 <sup>d</sup>	2051.5	23.5	19.4
Ru-1	0.6 <sup>c</sup>	3.9	5.3	83.4

<sup>a</sup>In CH<sub>3</sub>CN, 1.0 × 10<sup>-5</sup> M, 20 °C. <sup>b</sup>Upconversion quantum yields; measured with 2-iodo-boron-dipyrromethene as the standard ( $\Phi_F = 0.036$  in CH<sub>3</sub>CN). <sup>c</sup>Excited by a 473 nm laser. <sup>d</sup>Excited by a 532 nm laser. <sup>e</sup>Stern–Volmer quenching constants ( $K_{sv}$ ) of the quenching of lifetimes of the triplet excited states of Ir(III) complexes by perylene. <sup>f</sup>Bimolecular quenching constants ( $k_q$ ),  $K_{sv} = k_q \tau$ . <sup>g</sup>Delayed fluorescence lifetimes observed in the TTA upconversion with complexes as triplet photosensitizer and perylene as triplet acceptor.

may be responsible for the significant TTA upconversion than the other triplet photosensitizers. The data of a benchmark triplet photosensitizer for TTA upconversion,  $\text{Ru}(\text{dmb})_3[\text{PF}_6]_2$  (**Ru-1**), is also presented in Table 3 for comparison.

Upconversion is clearly visible with the unaided eye (Figure 13). For **Ir-2** and **Ir-3**, the emission color changed drastically

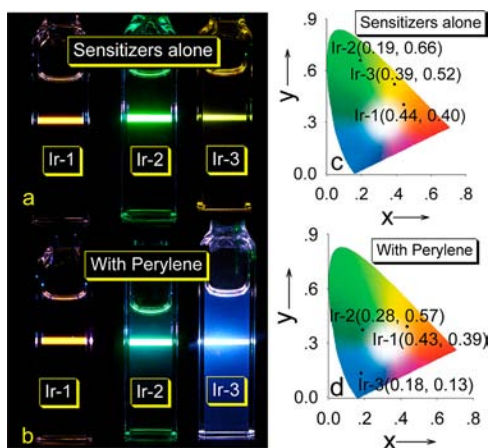
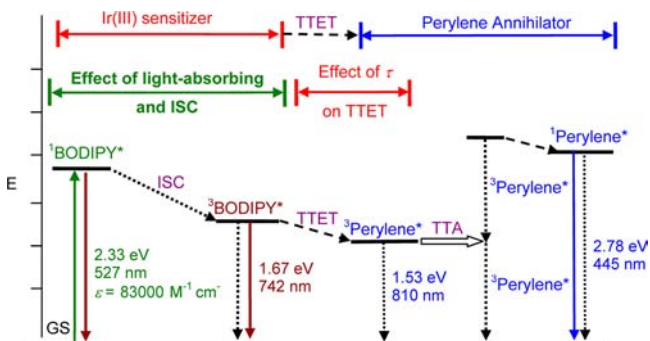


**Figure 13.** Photographs of the upconversions: (a) Ir(III) complexes alone; (b) upconversion (mixed solution with perylene). CIE diagram of (c) Ir(III) complexes alone and (d) in the presence of perylene (upconversion). **Ir-1** and **Ir-2** were excited by a 473 nm laser (5 mW), and **Ir-3** was excited by a 532 nm laser (5 mW).  $c = 1.0 \times 10^{-5}$  M in deaerated  $\text{CH}_3\text{CN}$  at 20 °C.

upon addition of triplet acceptor into the solution of the complexes. The color changes were quantified with the CIE coordinates (Figure 13c and 13d). For **Ir-1**, however, no emission color change was observed.

The mechanism of the TTA upconversion can be illustrated in Scheme 4. Upon excitation at the visible range (532 nm), the

#### Scheme 4. Qualitative Jablonski Diagram Illustrating the TTA Upconversion with Ir(III) Complexes (exemplified by **Ir-3**) as Triplet Photosensitizer and Perylene as Acceptor<sup>a</sup>



<sup>a</sup>The effect of the light-absorbing ability and triplet excited-state lifetime of the Ir(III) sensitizer on the efficiency of TTA upconversion is also shown. The wavelength of the laser used in the upconversion experiments is 532 nm. *E* is energy. GS is ground state ( $S_0$ ).  $^1\text{Bodipy}^*$  is intraligand singlet excited state (Bodipy localized). ISC is intersystem crossing.  $^3\text{Bodipy}^*$  is intraligand triplet excited state. TTET is triplet–triplet energy transfer.  $^3\text{Perylene}^*$  is the triplet excited state of perylene. TTA is triplet–triplet annihilation.  $^1\text{Perylene}^*$  is the singlet excited state of perylene. The typical power density of the laser used in the upconversion is  $70 \text{ mW cm}^{-2}$ , too low to observe simultaneous two-photon absorption.

$^1\text{Bodipy}^*$  singlet excited state is produced. Note that  $^1\text{Bodipy}^* \rightarrow ^1\text{MLCT}$  energy transfer is impossible due to the lower energy level of the  $^1\text{Bodipy}^*$  state than that of the  $^1\text{MLCT}$  state.  $^3\text{Bodipy}^*$  is produced by the ISC from the  $^1\text{Bodipy}^*$  state. The heavy-atom effect is crucial for the process. The triplet excited state of perylene was populated via the TTET between the triplet photosensitizer (Ir(III) complexes) and perylene. TTA of perylene as the triplet excited state will produce the singlet excited state. The radiative decay from the  $S_1$  state of perylene produced the delayed fluorescence, which has been proved by measurement of the luminescence lifetime (for **Ir-3**, the lifetime of the delayed fluorescence is 19.4  $\mu\text{s}$  vs 4.0 ns for the prompt fluorescence).

## CONCLUSION

We demonstrated the molecular designing method to enhance the effective visible-light absorption of Ir(III) complexes. Simply attaching an organic chromophore to the Ir(III) complex does not necessarily guarantee effective visible-light absorption, that is, the complex gives strong absorption of visible light but the excitation energy may be not efficiently transferred to the triplet excited state of the complex. In this case the strong absorption of the complex is useless. We proved that the  $\pi$  core of the light-harvesting organic chromophore must be connected to the Ir(III) coordination center via a conjugation linker, such as the  $-\text{C}\equiv\text{C}-$  bond. This strategy was proved by preparation of two cationic cyclometalated Ir(III) complexes ( $\text{PF}_6^-$  as the anions) with the Bodipy chromophore. Although both of the complexes show intense absorption of visible light, the complex (**Ir-3**) with direct connection of the  $\pi$  core of the visible-light-harvesting chromophore (Bodipy) to the coordination center shows weaker ligand fluorescence than the complex with connections at the meso phenyl of Bodipy (**Ir-2**). Furthermore, **Ir-3** shows RT phosphorescence of the Bodipy ligand at 742 nm, whereas no RT phosphorescence was observed for **Ir-2**. The Ir(III) complexes were used as triplet photosensitizers in two different triplet–triplet energy-transfer processes, i.e., photooxidation via the singlet oxygen ( $^1\text{O}_2$ ) photosensitizing and triplet–triplet annihilation (TTA) upconversion; both require a triplet excited state for initiation. **Ir-3** shows more efficient  $^1\text{O}_2$  sensitizing ( $^1\text{O}_2$  quantum yield  $\Phi_\Delta = 97\%$ ) and TTA upconversion (quantum yield  $\Phi_{\text{UC}} = 2.8\%$ ) than **Ir-2** ( $\Phi_\Delta = 52\%$ ,  $\Phi_{\text{UC}} = 1.2\%$ ). Therefore, the link of the  $\pi$  core of a visible-light-harvesting chromophore to the Ir(III) coordination center is an effective way to maximize the ISC effect, so that the excitation energy harvested by the chromophore can be efficiently funneled to the triplet excited state of the complexes. This information is useful for design of visible-light-absorbing transition metal complexes and application of these complexes in photocatalysis, photovoltaics, and TTA upconversions, etc.

## EXPERIMENTAL SECTION

**Analytical Measurements.** All chemicals are analytical pure and used as received. Solvents were dried and distilled for synthesis. 5-Ethynyl-2,2'-bipyridine,<sup>87</sup> 2-iodo-1,3,5,7-tetramethyl-8-phenyl-4,4-difluoro-4-bora-3a-azonia-4a-aza-s-indacene,<sup>86a</sup> and the cyclometalated Ir(III) chloro-bridge dimers  $[\text{Ir}(\text{ppy})_2]\text{Cl}_2$ <sup>59</sup> were synthesized according to literature methods; 1,3,5,7-tetramethyl-8-(4-bromophenyl)-4,4-difluoro-4-bora-3a-azonia-4a-aza-s-indacene was synthesized according to a modified literature method<sup>86a</sup> (see Supporting Information for molecular structural characterization data). **L2** and **L3** were synthesized by a Sonogashira coupling reaction using 5-ethynyl-2,2'-bipyridine and 1,3,5,7-tetramethyl-8-(4-bromophenyl)-



4,4-difluoro-4-bora-3a-azonia-4a-aza-s-indacene, 2-iodo-1,3,5,7-tetramethyl-8-phenyl-4,4-difluoro-4-bora-3a-azonia-4a-aza-s-indacene, respectively (see Supporting Information). Complexes **Ir-1**, **Ir-2**, and **Ir-3** were synthesized according to a modified method.<sup>32</sup>

NMR spectra were recorded on a 400 MHz Varian Unity Inova spectrophotometer. Mass spectra were recorded with Q-TOF Micro and MALDI micro MS spectrometers. Elemental analysis was carried out with VarioEL III Element analyzer (Elementar, Germany). Fluorescence quantum yields were measured with 2,6-diiodo-1,3,5,7-tetramethyl-8-phenyl-4,4-difluoroboradiazaindacene (2I-BDP) as standard ( $\Phi_F = 2.7\%$  in  $\text{CH}_3\text{CN}$ ).<sup>86a</sup> Phosphorescence quantum yields were measured with  $\text{Ru}(\text{dmb})_3[\text{PF}_6]_2$  ( $\Phi_P = 7.3\%$  in deaerated  $\text{CH}_3\text{CN}$ ) or 2I-BDP as the references.<sup>86a</sup> The emission spectra at 77 K were measured with a Oxford Optistat DN cryostat and FLS920 spectrofluorometer.

**Synthesis of Ir-1.**  $[\text{Ir}(\text{ppy})_2]\text{Cl}_2$  (53.6 mg, 0.05 mmol) and 2,2'-bipyridine (18.7 mg, 0.12 mmol) were dissolved in  $\text{CH}_2\text{Cl}_2/\text{MeOH}$  (12 mL, 2:1, v/v). Then the mixture was refluxed for 6 h under an argon atmosphere. The mixture was cooled to RT; a 10-fold excess of ammonium hexafluorophosphate was added. The suspension was stirred for 15 min and then filtered to remove insoluble inorganic salts. The solution was evaporated to dryness under reduced pressure to obtain a yellow solid. The crude product was further purified with column chromatography (silica gel, dichloromethane/methanol = 10:1, v/v); yellow solid was obtained (46.8 mg, yield 71.3%). <sup>1</sup>H NMR (400 MHz,  $\text{CDCl}_3/\text{CD}_3\text{OD}$ ):  $\delta$  8.49 (d, 4H,  $J = 7.8$  Hz), 8.18 (t, 1H,  $J = 9.0$  Hz), 7.94–7.87 (m, 6H), 7.78 (t, 1H,  $J = 7.8$  Hz), 7.70 (d, 1H,  $J = 7.3$  Hz), 7.52 (d, 1H,  $J = 7.8$  Hz), 7.42–7.36 (m, 6H), 7.07–7.00 (m, 2H), 6.94 (t, 1H,  $J = 7.1$  Hz), 6.31 (d, 1H,  $J = 7.6$  Hz). TOF MS ESI ( $\text{C}_{32}\text{H}_{24}\text{IrN}_4^+$ ): calcd  $m/z = 657.1630$ , found  $m/z = 657.1625$ . Anal. Calcd for  $\text{C}_{32}\text{H}_{24}\text{F}_6\text{IrN}_4\text{P}$ : C, 47.94; H, 3.02; N, 6.99. Found: C, 47.85; H, 3.05; N, 6.94.

**Synthesis of Ir-2.**  $[\text{Ir}(\text{ppy})_2]\text{Cl}_2$  (53.6 mg, 0.05 mmol) and **L2** (60.3 mg, 0.12 mmol) were dissolved in  $\text{CH}_2\text{Cl}_2/\text{MeOH}$  (12 mL, 2:1, v/v). Then the mixture was refluxed for 6 h under an argon atmosphere. After completion of the reaction, the mixture was cooled to RT; a 10-fold excess of ammonium hexafluorophosphate was added. The suspension was stirred for 15 min and then filtered to remove insoluble inorganic salts. The solution was evaporated to dryness under reduced pressure to obtain a crude yellow solid. Crude product was further purified with column chromatography (silica gel, dichloromethane/methanol = 15:1, v/v); a red solid was obtained (76.6 mg, 76.4%). <sup>1</sup>H NMR ( $\text{CDCl}_3$ , 400 MHz):  $\delta$  9.89 (d, 1H,  $J = 6.7$  Hz), 9.78 (d, 1H,  $J = 6.9$  Hz), 8.41 (d, 1H,  $J = 7.0$  Hz), 8.29 (t, 1H,  $J = 5.8$  Hz), 7.99–7.89 (m, 5H), 7.82–7.77 (m, 2H), 7.74–7.69 (m, 2H), 7.61 (d, 2H,  $J = 7.8$  Hz), 7.55–7.47 (m, 2H), 7.42 (t, 1H,  $J = 6.3$  Hz), 7.32 (d, 1H,  $J = 8.0$  Hz), 7.09–6.91 (m, 6H), 6.33–6.27 (m, 2H), 5.99 (s, 2H), 2.55 (s, 6H), 1.38 (s, 6H). <sup>13</sup>C NMR (100 MHz,  $\text{CDCl}_3$ ):  $\delta$  167.99, 167.87, 156.08, 155.60, 155.04, 151.77, 150.07, 148.57, 148.38, 143.53, 143.45, 142.96, 142.72, 140.38, 140.29, 138.35, 136.55, 132.76, 131.86, 131.69, 131.13, 131.02, 128.93, 128.59, 128.19, 127.67, 127.00, 125.11, 124.98, 124.44, 123.45, 122.87, 121.60, 121.43, 119.97, 119.89, 96.31, 85.54, 14.69. <sup>19</sup>F (376 MHz,  $\text{CDCl}_3$ ):  $\delta$  -146.55, -146.63, -146.72, -146.81. <sup>11</sup>B (128 MHz,  $\text{CDCl}_3$ ):  $\delta$  1.22, 0.97, 0.71. TOF MS ESI ( $\text{C}_{53}\text{H}_{41}\text{BF}_2\text{IrN}_6^+$ ): calcd  $m/z = 1003.3083$ , found  $m/z = 1003.3058$ . Anal. Calcd for  $\text{C}_{53}\text{H}_{41}\text{BF}_2\text{IrN}_6\text{P}$ : C, 55.45; H, 3.60; N, 7.32. Found: C, 55.41; H, 3.53; N, 7.34.

**Synthesis of Ir-3.**  $[\text{Ir}(\text{ppy})_2]\text{Cl}_2$  (53.6 mg, 0.05 mmol) and **L3** (55.3 mg, 0.11 mmol) were dissolved in  $\text{CH}_2\text{Cl}_2/\text{MeOH}$  (12 mL, 2:1, v/v). Then the mixture was refluxed for 6 h under argon. Thereafter the synthesis procedure is similar to that of **Ir-2**; a red solid was obtained (72.1 mg, 71.9%). <sup>1</sup>H NMR ( $\text{CDCl}_3$ , 400 MHz):  $\delta$  9.77–9.68 (m, 2H), 8.27–8.16 (m, 2H), 7.94–7.87 (m, 3H), 7.80–7.76 (m, 3H), 7.71–7.65 (m, 2H), 7.54–7.48 (m, 5H), 7.39 (t, 1H,  $J = 6.1$  Hz), 7.06–6.88 (m, 5H), 6.32–6.29 (m, 2H), 6.09 (s, 1H), 4.92 (s, 3H), 2.59 (d, 6H,  $J = 33.4$  Hz), 1.41 (d, 6H,  $J = 16.3$  Hz). <sup>13</sup>C NMR (100 MHz,  $\text{CDCl}_3$ ):  $\delta$  167.89, 159.76, 156.05, 155.73, 153.79, 151.52, 150.31, 150.23, 149.91, 148.56, 146.28, 143.51, 142.66, 142.56, 140.61, 140.33, 138.29, 138.24, 134.30, 133.31, 131.81, 130.93, 130.07, 129.56, 129.51, 127.79, 127.34, 126.80, 125.33, 124.95, 123.40, 123.12, 122.78,

119.94, 119.77, 91.51, 91.25, 15.03, 14.77, 13.45, 13.08. <sup>19</sup>F (376 MHz,  $\text{CDCl}_3$ ):  $\delta$  -146.43, -146.50, -146.59, -146.68. <sup>11</sup>B (128 MHz,  $\text{CDCl}_3$ ):  $\delta$  1.09, 0.84, 0.59. TOF MS ESI ( $\text{C}_{53}\text{H}_{41}\text{BF}_2\text{IrN}_6^+$ ): calcd  $m/z = 1003.3083$ , found  $m/z = 1003.3071$ . Anal. Calcd for  $\text{C}_{53}\text{H}_{41}\text{BF}_2\text{IrN}_6\text{P}$ : C, 55.45; H, 3.60; N, 7.32. Found: C, 55.45; H, 3.59; N, 7.33.

**Nanosecond Time-Resolved Transient Difference Absorption Spectroscopy.** Nanosecond time-resolved transient difference absorption spectra were recorded on a LP 920 laser flash photolysis spectrometer (Edinburgh Instruments, Livingston, U.K.). Samples were purged with  $\text{N}_2$  or argon for 30 min before measurement. Samples were excited with a 355 or 532 nm nanosecond pulsed laser, and transient signals were recorded on a Tektronix TDS 3012B oscilloscope.

**DFT Computational Methods.** Geometry optimizations were calculated using the B3LYP functional with the 6-31G(d)/LanL2DZ basis set.<sup>88</sup> The spin density of the triplet excited state was calculated with the energy minimized triplet geometries. Solvents were used in calculations (CPCM model). All calculations were performed using the Gaussian 09W software (Gaussian, Inc.).<sup>89</sup>

**Photooxidation.** A 35 W xenon lamp with a focusing reflector was used for photooxidation. The light power was measured with a solar power meter. The mixed solution of the complex (photosensitizer) and DHN was irradiated with 35 W xenon lamp (20 mW  $\text{cm}^{-2}$ ). Light with a wavelength shorter than 385 nm was blocked by 0.72 M  $\text{NaNO}_2$  solution. Photooxidation of DHN was recorded on the UV-vis spectrophotometer at intervals of 1–5 min depending on the efficiency of the sensitizer. DHN consumption was monitored by a decrease of the absorption at 301 nm, and the concentration of DHN was calculated using its molar absorption coefficient ( $\epsilon = 7664 \text{ M}^{-1} \text{ cm}^{-1}$ ).<sup>26</sup> Juglone production was monitored by an increase in the absorption at 427 nm. The concentration of juglone was calculated using its molar absorption coefficient ( $\epsilon = 3811 \text{ M}^{-1} \text{ cm}^{-1}$ ), and the yield of juglone was obtained by dividing the concentration of juglone with the initial concentration of DHN.<sup>26</sup> Photostability experiments were carried out using the same method.

**Singlet Oxygen (<sup>1</sup>O<sub>2</sub>) Quantum Yields ( $\Phi_\Delta$ ).**  $\Phi_\Delta$  values of the triplet photosensitizers were determined according to a modified literature method<sup>90</sup> with Rose Bengal (RB,  $\Phi_\Delta = 0.80$  in methanol) as the standard.<sup>91</sup> 1,3-Diphenylisobenzofuran (DPBF) was used as the <sup>1</sup>O<sub>2</sub> scavenger due to its fast reaction with <sup>1</sup>O<sub>2</sub>. The absorbance of DPBF was adjusted around 1.0 at 410 nm in air-saturated methanol. Then photosensitizer was added to the cuvette, and photosensitizer's absorbance was adjusted to around 0.2–0.3. Then we exposed the cuvette to monochromatic light at the specific wavelength for 10 or 20 s depending on the efficiency of the dye sensitizer. The irradiation wavelength for **Ir-1**, **Ir-2**, and **Ir-3** are 322 nm, 510 nm, and 537 nm, respectively. Absorbance was measured after each irradiation (six data points were collected). The slope of the curves of absorbance maxima of DPBF at 410 nm versus irradiation time for each photosensitizer were calculated. Singlet oxygen quantum yields ( $\Phi_\Delta$ ) were calculated according to the equation

$$\Phi_{\Delta\text{unk}} = \Phi_{\Delta\text{std}} \frac{m_{\text{unk}} F_{\text{std}}}{m_{\text{std}} F_{\text{unk}}} \quad (1)$$

where “unk” and “std” designate the “Ir(III) photosensitizers” and “RB”, respectively, “m” is the slope of the difference in the change in absorbance of DPBF (410 nm) with the irradiation time, and “F” is the absorption correction factor, which is given by  $F = 1 - 10^{-A}$  (A is absorption at the irradiation wavelength).

**TTA Upconversion.** A diode-pumped solid state laser was used for upconversions. The laser power was measured with a phototube. The mixed solution of the complex (triplet photosensitizer) and perylene (triplet acceptor) was degassed for at least 15 min with  $\text{N}_2$  or argon before measurement. Note, absorption of perylene at 532 nm is very weak; thus, the triplet acceptor cannot be excited by a 532 nm laser irradiation.

Upconversion quantum yields were determined with 2-iodo-1,3,5,7-tetramethyl-8-phenyl-4,4-difluoro-4-bora-3a-azonia-4a-aza-s-indacene

( $\Phi_F = 3.6\%$ , in  $\text{CH}_3\text{CN}$ ) as the standard.<sup>86a</sup> Upconversion quantum yields were calculated with a modified eq 2,<sup>77a</sup> where  $\Phi_{\text{unk}}$ ,  $I_{\text{unk}}$ , and  $\eta_{\text{unk}}$  represent the quantum yield, integrated photoluminescence intensity, and refractive index of the solutions. The equation is multiplied by a factor of 2 in order to make the maximum quantum yield unity.<sup>77a</sup> Furthermore, the absorption correction factor  $1 - 10^{-A}$  is used in the equation instead of the absorption ( $A$ ) due to the intense absorption of the samples compared to that of dilute solutions, which are normally used for determination of the luminescence quantum yields. The concentration of the sensitizers used in TTA upconversion is  $1.0 \times 10^{-5}$  M in  $\text{CH}_3\text{CN}$ , and absorption of the sample Ir-3 ( $A$  at 532 nm) used for determination of the upconversion quantum yields is 0.7623. Absorption of samples Ir-1 and Ir-2 ( $A$  at 473 nm) used for determination of the upconversion quantum yields is 0.0112 and 0.1913, respectively. Absorption of the standard 2-iodo-1,3,5,7-tetramethyl-8-phenyl-4,4-difluoro-4-bora-3a-azonia-4a-aza-*s*-indacene at 473 and 532 nm is 0.2035 and 0.0855, respectively.

$$\Phi_{\text{unk}} = 2\Phi_{\text{std}} \left( \frac{1 - 10^{-A_{\text{std}}}}{1 - 10^{-A_{\text{unk}}}} \right) \left( \frac{I_{\text{unk}}}{I_{\text{std}}} \right) \left( \frac{\eta_{\text{unk}}}{\eta_{\text{std}}} \right)^2 \quad (2)$$

The TTET efficiency was evaluated by Stern–Volmer quenching constants, the concentration of the sensitizer was at  $1.0 \times 10^{-5}$  M in  $\text{CH}_3\text{CN}$ , and the lifetimes of the triplet state of the photosensitizer were measured by LP920 with increasing perylene concentration.

Photographs of upconversion were taken with a Samsung NV 5 digital camera. CIE coordinates ( $x$ ,  $y$ ) of the emission of the sensitizers alone and emission of the upconversion were derived from emission spectra of TTA upconversion with the CIE Color Matching Linear Algebra software.

**Delayed Fluorescence of the Upconversion ( $\tau_{\text{DF}}$ ).** Delayed fluorescence ( $\tau_{\text{DF}}$ ) was measured with an Opolette 355II+UV nanosecond pulsed laser (typical pulse length 7 ns; pulse repetition 20 Hz; peak OPO energy, 4 mJ; wavelength is tunable in the range of 210–355 and 410–2200 nm; OPOTEK, USA), which is synchronized to the FLS 920 spectrofluorometer (Edinburgh, U.K.). The decay kinetics of the unconverted fluorescence (delayed fluorescence) was monitored with a FLS920 spectrofluorometer. The prompt fluorescence lifetime of the triplet acceptor perylene was measured with a EPL picosecond pulsed laser (405 nm), which is synchronized to the FLS 920 spectrofluorometer.

## ■ ASSOCIATED CONTENT

### ● Supporting Information

General experimental methods,  $^1\text{H}$ ,  $^{13}\text{C}$ ,  $^{19}\text{F}$ , and  $^{11}\text{B}$  NMR data, HRMS spectra of the compounds, and photophysical data of the complexes. This material is available free of charge via the Internet at <http://pubs.acs.org>.

## ■ AUTHOR INFORMATION

### Corresponding Author

\*E-mail: zhaojzh@dlt.edu.cn.

### Notes

The authors declare no competing financial interest.

## ■ ACKNOWLEDGMENTS

We thank the NSFC (20972024, 21073028, and 21273028), the Royal Society (UK) and NSFC China-UK Cost-Share Science Networks (21011130154), Science Foundation Ireland (SFI E.T.S. Walton Program 11/W.1/E2061), the Fundamental Research Funds for the Central Universities (DUT10ZD212), the Ministry of Education (NCET-08-0077 and 20120041130005), and Dalian University of Technology for financial support.

## ■ REFERENCES

- (a) Chan, S.-C.; Chan, M. C. W.; Wang, Y.; Che, C.-M.; Cheung, K.-K.; Zhu, N. *Chem.—Eur. J.* **2001**, *7*, 4180–4190. (b) Huo, S.; Deaton, J. C.; Rajeswaran, M.; Lenhart, W. *Inorg. Chem.* **2006**, *45*, 3155–3157.
- (a) Chou, P. T.; Chi, Y. *Chem.—Eur. J.* **2007**, *13*, 380–395. (b) Chou, P. T.; Chi, Y.; Chung, M.-W.; Lin, C.-C. *Coord. Chem. Rev.* **2011**, *255*, 2653–2665.
- (a) Flamigni, L.; Barbieri, A.; Sabatini, C.; Ventura, B.; Barigelletti, F. *Top. Curr. Chem.* **2007**, *281*, 143–203. (b) Yersin, H.; Rausch, A. F.; Czerwieńiec, R.; Hofbeck, T.; Fischer, T. *Coord. Chem. Rev.* **2011**, *255*, 2622–2652.
- Du, B.; Wang, L.; Wu, H.; Yang, W.; Zhang, Y.; Liu, R.; Sun, M.; Peng, J.; Cao, Y. *Chem.—Eur. J.* **2007**, *13*, 7432–7442.
- Orselli, E.; Albuquerque, R. Q.; Franssen, P. M.; Fröhlich, R.; Janssen, H. M.; Cola, L. D. *J. Mater. Chem.* **2008**, *18*, 4579–4590.
- Song, Y. H.; Chiu, Y. C.; Chi, Y.; Cheng, Y. M.; Lai, C. H.; Chou, P. T.; Wong, K. T.; Tsai, M. H.; Wu, C. C. *Chem.—Eur. J.* **2008**, *14*, 5423–5434.
- (a) Zhou, G.; Ho, C. L.; Wong, W. Y.; Wang, Q.; Ma, D.; Wang, L.; Lin, Z.; Marder, T. B.; Beeby, A. *Adv. Funct. Mater.* **2008**, *18*, 499–511. (b) Wong, W.-Y.; Ho, C.-L. *Coord. Chem. Rev.* **2009**, *253*, 1709–1758.
- He, L.; Qiao, J.; Duan, L.; Dong, G.; Zhang, D.; Wang, L.; Qiu, Y. *Adv. Funct. Mater.* **2009**, *19*, 2950–2960.
- (a) Du, B. S.; Lin, C. H.; Chi, Y.; Hung, J. Y.; Chung, M. W.; Lin, T. Y.; Lee, G. H.; Wong, K. T.; Chou, P. T.; Hung, W. Y.; Chiu, H. C. *Inorg. Chem.* **2010**, *49*, 8713–8723. (b) Guo, F.; Sun, W.; Liu, Y.; Schanze, K. *Inorg. Chem.* **2005**, *44*, 4055–4065.
- Chi, Y.; Chou, P. T. *Chem. Soc. Rev.* **2010**, *39*, 638–655.
- Peng, T.; Yang, Y.; Liu, Y.; Ma, D.; Hou, Z.; Wang, Y. *Chem. Commun.* **2011**, *47*, 3150–3152.
- Baranoff, E.; Orselli, E.; Allouche, L.; Censo, D. D.; Scopelliti, R.; Grätzel, M.; Nazeeruddin, M. K. *Chem. Commun.* **2011**, *47*, 2799–2801.
- (a) Kozhevnikov, D. N.; Kozhevnikov, V. N.; Shafikov, M. Z.; Prokhorov, A. M.; Bruce, D. W.; Williams, J. A. G. *Inorg. Chem.* **2011**, *50*, 3804–3815. (b) Tang, W.-S.; Lu, X.-X.; Wong, K. M.-C.; Yam, V. W. W. *J. Mater. Chem.* **2005**, *15*, 2714–2720. (c) Ko, C.-C.; Yam, V. W.-W. *J. Mater. Chem.* **2010**, *20*, 2063–2070. (d) Tanaka, Y.; Wong, K. M.-C.; Yam, V. W.-W. *Chem. Sci.* **2012**, *3*, 1185–1191.
- Kuwabara, J.; Namekawa, T.; Haga, M.; Kanbara, T. *Dalton Trans.* **2012**, *41*, 44–46.
- Lo, K. K. W.; Chung, C. K.; Lee, T. K. M.; Lui, L. H.; Tsang, K. H. K.; Zhu, N. *Inorg. Chem.* **2003**, *42*, 6886–6897.
- Borisov, S. M.; Klimant, I. *Anal. Chem.* **2007**, *79*, 7501–7509.
- Zhao, Q.; Li, F.; Huang, C. *Chem. Soc. Rev.* **2010**, *39*, 3007–3030.
- (a) Fernández-Moreira, V.; Thorp-Greenwood, F. L.; Coogan, M. P. *Chem. Commun.* **2010**, *46*, 186–202. (b) Zhou, Y.; Yoon, J. *Chem. Soc. Rev.* **2012**, *41*, 52–67.
- Murphy, L.; Congreve, A.; Pålsson, L. O.; Williams, J. A. G. *Chem. Commun.* **2010**, *46*, 8743–8745.
- Xie, Z.; Ma, L.; DeKrafft, K. E.; Jin, A.; Lin, W. J. *Am. Chem. Soc.* **2010**, *132*, 922–923.
- Tian, N.; Lenkeit, D.; Pelz, S.; Fischer, L. H.; Escudero, D.; Schiewek, R.; Klink, D.; Schmitz, O. J.; González, L.; Schäferling, M.; Holder, E. *Eur. J. Inorg. Chem.* **2010**, 4875–4885.
- Koren, K.; Borisov, S. M.; Saf, R.; Klimant, I. *Eur. J. Inorg. Chem.* **2011**, 1531–1534.
- Zanarini, S.; Felici, M.; Valenti, G.; Marcaccio, M.; Prodi, L.; Bonacchi, S.; Contreras-Carballada, P.; Williams, R. M.; Feiters, M. C.; Nolte, R. J. M.; Cola, L. D.; Paolucci, F. *Chem.—Eur. J.* **2011**, *17*, 4640–4647.
- (a) Goldsmith, J. I.; Hudson, W. R.; Lowry, M. S.; Anderson, T. H.; Bernhard, S. *J. Am. Chem. Soc.* **2005**, *127*, 7502–7510. (b) DiSalle, B. F.; Bernhard, S. *J. Am. Chem. Soc.* **2011**, *133*, 11819–11821. (c) Takizawa, S.-y.; Pérez-Bolívar, C.; Anzenbacher, P., Jr.; Murata, S. *Eur. J. Inorg. Chem.* **2012**, 3975–3979. (d) Yuan, Y.-J.; Zhang, J.-Y.; Yu,

- Z.-T.; Feng, J.-Y.; Luo, W.-J.; Ye, J.-H.; Zou, Z.-G. *Inorg. Chem.* **2012**, *51*, 4123–4133.
- (25) Lowry, M. S.; Bernhard, S. *Chem.—Eur. J.* **2006**, *12*, 7970–7977.
- (26) Takizawa, S.; Aboshi, R.; Murata, S. *Photochem. Photobiol. Sci.* **2011**, *10*, 895–903.
- (27) (a) Geiß, B.; Lambert, C. *Chem. Commun.* **2009**, 1670–1672. (b) Hofbeck, T.; Yersin, H. *Inorg. Chem.* **2010**, *49*, 9290–9299.
- (28) Hanss, D.; Freys, J. C.; Bernardinelli, G.; Wenger, O. S. *Eur. J. Inorg. Chem.* **2009**, 4850–4859.
- (29) Li, Y.; Liu, Y.; Zhou, M. *Dalton Trans.* **2012**, *41*, 2582–2591.
- (30) Bronner, C.; Veiga, M.; Guenet, A.; Cola, L. D.; Hosseini, M. W.; Strassert, C. A.; Baudron, S. A. *Chem.—Eur. J.* **2012**, *18*, 4041–4050.
- (31) Zhao, W.; Castellano, F. N. *J. Phys. Chem. A* **2006**, *110*, 11440–11445.
- (32) Sun, J.; Wu, W.; Guo, H.; Zhao, J. *Eur. J. Inorg. Chem.* **2011**, 3165–3173.
- (33) Zhao, J.; Ji, S.; Guo, H. *RSC Adv.* **2011**, *1*, 937–950.
- (34) Liu, S.; Zhao, Q.; Fan, Q.; Huang, W. *Eur. J. Inorg. Chem.* **2008**, 2177–2185.
- (35) Ragni, R.; Orselli, E.; Kottas, G. S.; Omar, O. H.; Babudri, F.; Pedone, A.; Naso, F.; Farinola, G. M.; Cola, L. D. *Chem.—Eur. J.* **2009**, *15*, 136–148.
- (36) Hallett, A. J.; Kariuki, B. M.; Pope, S. J. A. *Dalton Trans.* **2011**, *40*, 9474–9481.
- (37) Baranoff, E.; Fantacci, S.; Angelis, F. D.; Zhang, X.; Scopelliti, R.; Grätzel, M.; Nazeeruddin, M. K. *Inorg. Chem.* **2011**, *50*, 451–462.
- (38) (a) Yan, Q.; Fan, Y.; Zhao, D. *Macromolecules* **2012**, *45*, 133–141. (b) Chen, J.-S.; Zhao, G.-J.; Cook, T. R.; Sun, X.-F.; Yang, S.-Q.; Zhang, M.-X.; Han, K.-L.; Stang, P. J. *J. Phys. Chem. A* **2012**, *116*, 9911–9918.
- (39) Gärtner, F.; Cozzula, D.; Losse, S.; Boddien, A.; Anilkumar, G.; Junge, H.; Schulz, T.; Marquet, N.; Spannenberg, A.; Gladiali, S.; Beller, M. *Chem.—Eur. J.* **2011**, *17*, 6998–7006.
- (40) Gärtner, F.; Denurra, S.; Losse, S.; Neubauer, A.; Boddien, A.; Gopinathan, A.; Spannenberg, A.; Junge, H.; Lochbrunner, S.; Blug, M.; Hoch, S.; Busse, J.; Gladiali, S.; Beller, M. *Chem.—Eur. J.* **2012**, *18*, 3220–3225.
- (41) Wang, X.; Jia, J.; Huang, Z.; Zhou, M.; Fei, H. *Chem.—Eur. J.* **2011**, *17*, 8028–8032.
- (42) (a) Edkins, R. M.; Bettington, S. L.; Goeta, A. E.; Beeby, A. *Dalton Trans.* **2011**, *40*, 12765–12770. (b) McCusker, C. E.; Hablot, D.; Ziessel, R.; Castellano, F. N. *Inorg. Chem.* **2012**, *51*, 7957–7959.
- (43) Zhao, J.; Ji, S.; Wu, W.; Guo, H.; Sun, J.; Sun, H.; Liu, Y.; Li, Q.; Huang, L. *RSC Adv.* **2012**, *2*, 1712–1728.
- (44) Hanson, K.; Tamayo, A.; Diev, V. V.; Whited, M. T.; Djurovich, P. I.; Thompson, M. E. *Inorg. Chem.* **2010**, *49*, 6077–6084.
- (45) Liu, Y.; Wu, W.; Zhao, J.; Zhang, X.; Guo, H. *Dalton Trans.* **2011**, *40*, 9085–9089.
- (46) Sun, H.; Guo, H.; Wu, W.; Liu, X.; Zhao, J. *Dalton Trans.* **2011**, *40*, 7834–7841.
- (47) Wu, W.; Zhao, J.; Guo, H.; Sun, J.; Ji, S.; Wang, Z. *Chem.—Eur. J.* **2012**, *18*, 1961–1968.
- (48) (a) Galletta, M.; Campagna, S.; Quesada, M.; Ulrich, G.; Ziessel, R. *Chem. Commun.* **2005**, 4222–4224. (b) Nastasi, F.; Puntoriero, F.; Campagna, S.; Olivier, J.-H.; Ziessel, R. *Phys. Chem. Chem. Phys.* **2010**, *12*, 7392–7402.
- (49) Rachford, A. A.; Ziessel, R.; Bura, T.; Retailleau, P.; Castellano, F. N. *Inorg. Chem.* **2010**, *49*, 3730–3736.
- (50) Wu, W.; Ji, S.; Wu, W.; Shao, J.; Guo, H.; James, T. D.; Zhao, J. *Chem.—Eur. J.* **2012**, *18*, 4953–4964.
- (51) (a) Loudet, A.; Burgess, K. *Chem. Rev.* **2007**, *107*, 4891–4932. (b) Ulrich, G.; Ziessel, R.; Harriman, A. *Angew. Chem., Int. Ed.* **2008**, *47*, 1184–1201. (c) Benniston, A. C.; Copley, G. *Phys. Chem. Chem. Phys.* **2009**, *11*, 4124–4131. (c) Ziessel, R.; Harriman, A. *Chem. Commun.* **2011**, *47*, 611–631.
- (52) Zhang, X.; Xiao, Y.; Qian, X. *Org. Lett.* **2008**, *10*, 29–32.
- (53) (a) Gabe, Y.; Urano, Y.; Kikuchi, K.; Kojima, H.; Nagano, T. *J. Am. Chem. Soc.* **2004**, *126*, 3357–3367. (b) Sunahara, H.; Urano, Y.; Kojima, H.; Nagano, T. *J. Am. Chem. Soc.* **2007**, *129*, 5597–5604. (c) Yogo, T.; Urano, Y.; Mizushima, A.; Sunahara, H.; Inoue, T.; Hirose, K.; Iino, M.; Kikuchi, K.; Nagano, T. *Proc. Natl. Acad. Sci. U.S.A.* **2008**, *105*, 28–32. (d) Yogo, T.; Urano, Y.; Ishitsuka, Y.; Maniwa, F.; Nagano, T. *J. Am. Chem. Soc.* **2005**, *127*, 12162–12163.
- (54) Wang, D.; Fan, J.; Gao, X.; Wang, B.; Sun, S.; Peng, X. *J. Org. Chem.* **2009**, *74*, 7675–7683.
- (55) Gorman, A.; Killoran, J.; O’Shea, C.; Kenna, T.; Gallagher, W. M.; O’Shea, D. F. *J. Am. Chem. Soc.* **2004**, *126*, 10619–10631.
- (56) (a) Coskun, A.; Akkaya, E. U. *J. Am. Chem. Soc.* **2005**, *127*, 10464–10465. (b) Bozdemir, O. A.; Erbas-Cakmak, S.; Ekiz, O.; Dana, A.; Akkaya, E. U. *Angew. Chem., Int. Ed.* **2011**, *50*, 10907–10912. (c) Coskun, A.; Akkaya, E. U. *J. Am. Chem. Soc.* **2006**, *128*, 14474–14475. (d) Guliyev, R.; Coskun, A.; Akkaya, E. U. *J. Am. Chem. Soc.* **2009**, *131*, 9007–9013.
- (57) (a) Lu, H.; Shimizu, S.; Mack, J.; Shen, Z.; Kobayashi, N. *Chem. Asian J.* **2011**, *6*, 1026–1037. (b) Wang, Y.-W.; Descalzo, A. B.; Shen, Z.; You, X.-Z.; Rurack, K. *Chem.—Eur. J.* **2012**, *18*, 7306–7309.
- (58) Cao, J.; Zhao, C.; Feng, P.; Zhang, Y.; Zhu, W. *RSC Adv.* **2012**, *2*, 418–420.
- (59) Lowry, M. S.; Hudson, W. R.; Pascal, R. A.; Bernhard, S. *J. Am. Chem. Soc.* **2004**, *126*, 14129–14135.
- (60) Rachford, A. A.; Goeb, S.; Castellano, F. N. *J. Am. Chem. Soc.* **2008**, *130*, 2766–2767.
- (61) Wu, W.; Wu, W.; Ji, S.; Guo, H.; Zhao, J. *Dalton Trans.* **2011**, *40*, 5953–5963.
- (62) Lamansky, S.; Djurovich, P.; Murphy, D.; Abdel-Razzaq, F.; Lee, H. E.; Adachi, C.; Burrows, P. E.; Forrest, S. R.; Thompson, M. E. *J. Am. Chem. Soc.* **2001**, *123*, 4304–4312.
- (63) Ruggi, A.; Alonso, M. B.; Reinhoudt, D. N.; Velders, A. H. *Chem. Commun.* **2010**, *46*, 6726–6728.
- (64) Mak, C. S. K.; Pentlehner, D.; Stich, M.; Wolfbeis, O. S.; Chan, W. K.; Yersin, H. *Chem. Mater.* **2009**, *21*, 2173–2175.
- (65) Hisamatsu, Y.; Aoki, S. *Eur. J. Inorg. Chem.* **2011**, 5360–5369.
- (66) Turro, N. J.; Ramamurthy, V.; Scaiano, J. C. *Principles of Molecular Photochemistry: An Introduction*; University Science Books: Sausalito, CA, 2009.
- (67) Armaroli, N. *ChemPhysChem* **2008**, *9*, 371–373.
- (68) Ji, S.; Wu, W.; Song, P.; Han, K.; Wang, Z.; Liu, S.; Guo, H.; Zhao, J. *J. Mater. Chem.* **2010**, *20*, 1953–1963.
- (69) Liu, Y.; Zhao, J. *Chem. Commun.* **2012**, *48*, 3751–3753.
- (70) Sun, J.; Zhao, J.; Guo, H.; Wu, W. *Chem. Commun.* **2012**, *48*, 4169–4171.
- (71) Benites, J. A.; Valderrama; Karina Bettega, R. C.; Pedrosa, P. B.; Calderon, J. Verrax. *Eur. J. Med. Chem.* **2010**, *45*, 6052–6057.
- (72) Keivanidis, P. E.; Balushev, S. *Adv. Mater.* **2003**, *15*, 2095–2098.
- (73) Monguzzi, A.; Mezyk, J.; Scotognella, F.; Tubino, R.; Meinar, F. *Phys. Rev. B: Condens. Matter Phys.* **2008**, *78*, 195112.
- (74) Balushev, S.; Yakutkin, V.; Miteva, T.; Wegner, G.; Roberts, T.; Nelles, G.; Yasuda, A.; Chernov, S.; Aleshchenkov, S.; Cheprakov, A. *New J. Phys.* **2008**, *10*, 013007.
- (75) Chen, H. C.; Hung, C. Y.; Wang, K. H.; Chen, H. L.; Fann, W. S.; Chien, F. C.; Chen, P.; Chow, T. J.; Hsu, C. P.; Sun, S. S. *Chem. Commun.* **2009**, 4064–4066.
- (76) (a) Cheng, Y. Y.; Khoury, T.; Clady, R. G. C. R.; Tayebjee, M. J. Y.; Ekins-Daukes, N. J.; Crossley, M. J.; Schmidt, T. W. *Phys. Chem. Chem. Phys.* **2010**, *12*, 66–71. (b) Cheng, Y. Y.; Fückel, B.; Khoury, T.; Clady, R. G. C. R.; Ekins-Daukes, N. J.; Crossley, M. J.; Schmidt, T. W. *J. Phys. Chem. A* **2011**, *115*, 1047–1053. (c) Liu, Q.; Yang, T.; Feng, W.; Li, F. *J. Am. Chem. Soc.* **2012**, *134*, 5390–5397.
- (77) (a) Rachford, T. N. S.; Castellano, F. N. *Coord. Chem. Rev.* **2010**, *254*, 2560–2573. (b) Singh-Rachford, T. N.; Castellano, F. N. *Inorg. Chem.* **2009**, *48*, 2541–2548. (c) Singh-Rachford, T. N.; Nayak, A.; Muro-Small, M. L.; Goeb, S.; Therien, M. J.; Castellano, F. N. *J. Am. Chem. Soc.* **2010**, *132*, 14203–14211. (d) Singh-Rachford, T. N.; Castellano, F. N. *J. Phys. Chem. Lett.* **2010**, *1*, 195–200.

- (78) Ceroni, P. *Chem.—Eur. J.* **2011**, *17*, 9560–9564.
- (79) Monguzzi, A.; Tubino, R.; Hoseinkhani, S.; Campione, M.; Meinardi, F. *Phys. Chem. Chem. Phys.* **2012**, *14*, 4322–4332.
- (80) (a) Cheng, Y. Y.; Fückel, B.; MacQueen, R. W.; Khoury, T.; Clady, R. G. R. C.; Schulze, T. F.; Ekins-Daukes, N. J.; Crossley, M. J.; Stannowski, B.; Lips, K.; Schmidt, T. *Energy Environ. Sci.* **2012**, *5*, 6953–6959. (b) Borisov, S. M.; Larndorfer, C.; Klimant, I. *Adv. Funct. Mater.* **2012**, *22*, 4360–4368. (c) Zhang, C.; Zheng, J. Y.; Zhao, Y. S.; Yao, J. *Adv. Mater.* **2011**, *23*, 1380–1384.
- (81) Kim, H. M.; Cho, B. R. *Acc. Chem. Res.* **2009**, *42*, 863–872.
- (82) Lüthi, S. R.; Pollnau, M.; Güdel, H. U. *Phys. Rev. B.* **1999**, *60*, 162–178.
- (83) Wenger, O. S.; Güdel, H. U. *Inorg. Chem.* **2001**, *40*, 5747–5753.
- (84) (a) Liu, Q.; Sun, Y.; Yang, T.; Feng, W.; Li, C.; Li, F. *J. Am. Chem. Soc.* **2011**, *133*, 17122–17125. (b) Zhou, J.; Liu, Z.; Li, F. *Chem. Soc. Rev.* **2012**, *41*, 1323–1349.
- (85) Haase, M.; Schäfer, H. *Angew. Chem., Int. Ed.* **2011**, *50*, 5808–5829.
- (86) (a) Wu, W.; Guo, H.; Wu, W.; Ji, S.; Zhao, J. *J. Org. Chem.* **2011**, *76*, 7056–7064. (b) Wu, W.; Zhao, J.; Sun, J.; Guo, S. *J. Org. Chem.* **2012**, *77*, 5305–5312. (c) Guo, S.; Wu, W.; Guo, H.; Zhao, J. *J. Org. Chem.* **2012**, *77*, 3933–3943. (d) Xiong, L.; Chen, Z.; Tian, Q.; Cao, T.; Xu, C.; Li, F. *Anal. Chem.* **2009**, *81*, 8687–8694.
- (87) Pefkianakis, E. K.; Tzanetos, N. P.; Kallitsis, J. K. *Chem. Mater.* **2008**, *20*, 6254–6262.
- (88) (a) Becke, A. D. *J. Chem. Phys.* **1993**, *98*, 5648–5652. (b) Ditchfield, R.; Hehre, W. J.; Pople, J. A. *J. Chem. Phys.* **1971**, *54*, 724–728.
- (89) Frisch, M. J.; Trucks, G. W.; Schlegel, H. B.; Scuseria, G. E.; Robb, M. A.; Cheeseman, J. R.; Scalmani, G.; Barone, V.; Mennucci, B.; Petersson, G. A.; Nakatsuji, H.; Caricato, M.; Li, X.; Hratchian, H. P.; Izmaylov, A. F.; Bloino, J.; Zheng, G.; Sonnenberg, J. L.; Hada, M.; Ehara, M.; Toyota, K.; Fukuda, R.; Hasegawa, J.; Ishida, M.; Nakajima, T.; Honda, Y.; Kitao, O.; Nakai, H.; Vreven, T.; Montgomery, J. A., Jr.; Peralta, J. E.; Ogliaro, F.; Bearpark, M.; Heyd, J. J.; Brothers, E.; Kudin, K. N.; Staroverov, V. N.; Kobayashi, R.; Normand, J.; Raghavachari, K.; Rendell, A.; Burant, J. C.; Iyengar, S. S.; Tomasi, J.; Cossi, M.; Rega, N.; Millam, N. J.; Klene, M.; Knox, J. E.; Cross, J. B.; Bakken, V.; Adamo, C.; Jaramillo, J.; Gomperts, R.; Stratmann, R. E.; Yazyev, O.; Austin, A. J.; Cammi, R.; Pomelli, C.; Ochterski, J. W.; Martin, R. L.; Morokuma, K.; Zakrzewski, V. G.; Voth, G. A.; Salvador, P.; Dannenberg, J. J.; Dapprich, S.; Daniels, A. D.; Farkas, Ö.; Foresman, J. B.; Ortiz, J. V.; Cioslowski, J.; Fox, D. J. *Gaussian 09*, revision A.1; Gaussian Inc.: Wallingford, CT, 2009.
- (90) Adarsh, N.; Avirah, R.; Ramaiah, D. *Org. Lett.* **2010**, *12*, 5720–5723.
- (91) Wilkinson, F.; Helman, W. P.; Ross, A. B. *J. Phys. Chem. Ref. Data* **1993**, *22*, 113–262.